Nuclear Physics B119 (1977) 362–400

PARTIAL-WAVE ANALYSES OF $\bar{K}N$ TWO-BODY REACTIONS BETWEEN 1480 AND 2170 MeV

Rutherford Laboratory – Imperial College Collaboration

G.P. GOPAL, R.T. ROSS, A.J. VAN HORN * and A.C. McPHERSON
Rutherford Laboratory

E.F. CLAYTON, T.C. BACON and I. BUTTERWORTH
Imperial College, London

Received 26 August 1976
(Revised 26 November 1976)

We present partial-wave analyses of the reactions $\bar{K}N \to \bar{K}N$, $\bar{K}N \to \Sigma\pi$, $\bar{K}N \to \Lambda\pi$, using world data from 1480 to 2170 MeV c.m. energy including new data in the range 1775 to 1960 MeV. The three channels have been treated in parallel using energy-dependent partial-wave analysis techniques.

1. Introduction

We have obtained partial waves for the reactions

$$\bar{K}N \to \bar{K}N$$
$$\to \Sigma\pi$$
$$\to \Lambda\pi$$

over the c.m. energy range 1480–2170 MeV. This work differs from previous analyses in several aspects.

(a) By fitting over the complete energy range for which data are available we avoid the problems of energy continuation that are inherent in shorter range fits. In particular using preliminary data [1] from 1480 to 1530 MeV our solutions continue onto the region of the established D03(1520) resonance, which constraints the low waves of the solution.

(b) By performing parallel single-channel analyses we attempt to obtain consis-

* Present address: Harvard University, Department of Physics, Cambridge, Massachusetts 02138, USA.

tent resonance parameters in all three channels, but allow independent backgrounds in each channel.

(c) We have selected a consistent set of the most recent data (including our new data in the region 1775–1960 MeV) [2].

2. The data

In general we have selected data from the most recent and highest statistics experiment in any given energy range. In regions where these experiments overlap, they are generally consistent and data from only one of these were used. The data fitted were the following:

2.1. The $\bar{K}N$ channel

(a) Cross sections and angular distributions of $K^-p \to K^-p$ at 66 momenta between 0.285 and 1.843 GeV/c.

(b) Cross sections and angular distributions of $K^-p \to \bar{K}^0n$ at 64 momenta between 0.285 and 1.843 GeV/c.

(c) Polarisations of $K^-p \to K^-p$ at 25 momenta (all available data) between 0.865 and 1.732 GeV/c.

(d) Interpolated K^-p and $I = 1$ and $I = 0$ total cross sections at 53 momenta between 0.415 and 1.843 GeV/c. The quoted errors on $I = 1$ and $I = 0$ cross sections have been increased by a factor of two, since these data are unpublished and both have been fitted in addition to the K^-p total cross section [3].

(e) Ratios of the real to imaginary part of the forward elastic scattering amplitude at the same momenta as (d), the values being interpolated from the dispersion relation calculation of ref. [4]. The error assigned to each point was that of the nearest measured point used in these calculations.

2.2. The $\Sigma\pi$ channel

(a) Cross sections and angular distributions of $K^-p \to \Sigma^+\pi^-$ at 68 momenta between 0.295 and 1.843 GeV/c.

(b) Cross sections and angular distributions of $K^-p \to \Sigma^-\pi^+$ at the same momenta as (a).

(c) Polarisations of $K^-p \to \Sigma^+\pi^-$ in terms of the associated Legendre expansion coefficients B_l/A_0 at the same momenta *. In the $\Sigma^\pm\pi^\mp$ channels above 1.4 GeV/c both CRS and LBL data [5,6] were used since they are of similar statistics.

* A_l and B_l are the coefficients of the usual Legendre expansions:

$$\frac{d\sigma}{d\Omega} = \lambda\!\!\!^{-2} \sum_l A_l P_l(\cos\theta)\,, \qquad P\frac{d\sigma}{d\Omega} = \hat{n}\lambda\!\!\!^{-2} \sum_l B_l P_l^1(\cos\theta)\,,$$

where the parameters are as defined in sect. 3.

Table 1
The data used in this analysis and the χ^2 contributions given as χ^2/data point from the best solutions in each channel as described in text

Charge state	Data type	Momentum range (GeV/c)	C.m. energy range (MeV)	Expt.	No. of momenta	No. of data points (N)	χ^2/N
(a) $\bar{K}N$							
elastic	$A_0, A_I/A_0$	0.285–0.435	1481–1536	Tripp [1]	16	72	2.49
	$d\sigma/d\Omega$	0.455–0.793	1544–1696	CHS [13]	18	577	0.98
		0.806–0.935	1702–1763	Ch-H [10]	8	275	0.86
		0.960–1.355	1775–1957	RL-IC [2]	11	440	1.04
		1.367–1.843	1963–2169	CHM [10] a)	13	450	1.10
				total	66	1814	1.07
	P	0.862–1.784	1729–2144	refs. [16]	25	612	1.09
$\bar{K}^0n$	$A_0, A_I/A_0$	0.285–0.435	1481–1536	Tripp [1]	16	71	1.44
	$d\sigma/d\Omega$	0.455–0.838	1544–1717	CHS [13]	20	298	1.26
		0.862–0.936	1729–1764	Ch-LBL [14]	4	131	1.07
		0.960–1.355	1775–1957	RL-IC [2]	11	205	1.40
		1.367–1.843	1963–2169	CHM [10] a)	13	211	1.24
				total	64	916	1.28
total cross sections	σ_{K^-p}	0.415–1.843	1528–2169	Kycia [3] Bugg	50 interpolated points	50	1.38
	$\sigma_{I=0}$ and $\sigma_{I=1}$	as above				100 b)	1.62
	$\mathrm{Re}(f(0))/\mathrm{Im}(f(0))$ dispersion relation from ref. [4]					50 b)	0.13
				overall		3542	1.13
				with approximately 160 parameters			
(b) $\Sigma\pi$							
$\Sigma^+\pi^-$	$A_0, A_I/A_0$	0.295–0.435	1484–1536	Tripp [1]	15	69	1.28
	$d\sigma/d\Omega$	0.455–0.838	1544–1717	CHS [13]	20	329	0.98
		0.862–0.936	1729–1763	Ch-LBL [14]	6	178	1.09
		0.960–1.355	1775–1957	RL-IC [2]	11	189	1.16
		1.368–1.843	1963–2169	CRS [5]	11	160	1.13
		1.453–1.694	2001–2106	LBL [6]	5	71	0.91
				total	68	996	1.08
$\Sigma^+\pi^-$	B_I/A_0	0.295–0.435	1484–1536	Tripp [1]	15	57	1.06
		0.455–0.838	1544–1717	CHS [13]	20	82	1.57
		0.862–0.936	1729–1763	Ch-LBL [14]	6	36	1.76
		0.960–1.355	1775–1957	RL-IC [2]	11	84	1.10
		1.368–1.843	1963–2169	CRS [5]	11	77	1.20
		1.453–1.694	2001–2106	LBL [6]	5	35	1.05
				total	68	371	1.27

Table 1 (continued)

Charge state	Data type	Momentum range (GeV/c)	C.m. energy range (MeV)	Expt.	No. of momenta	No. of data points (N)	χ^2/N
(b) $\Sigma\pi$ (continued)							
$\Sigma^-\pi^+$	$A_0, A_l/A_0$	0.295–0.435	1484–1536	Tripp [1]	15	72	1.10
	$d\sigma/d\Omega$	0.455–0.838	1544–1717	CHS [13]	20	316	1.01
		0.862–0.936	1729–1763	Ch-LBL [14]	6	164	1.18
		0.960–1.355	1775–1957	RL-IC [2]	11	197	1.09
		1.368–1.843	1963–2169	CRS [5]	11	124	1.21
		1.453–1.694	2001–2106	LBL [6]	5	55	0.99
				total	68	928	1.09
$\Sigma^0\pi^+$	$d\sigma/d\Omega$	0.320–0.790	1491–1695	BEGPR [7]	11	139	1.04
	B_l/A_0	0.320–0.790	1491–1695	BEGPR [7]	11	40	1.15
$\Sigma^0\pi^0$	A_l/A_0	0.295–0.435	1484–1536	Tripp [1]	15	60	1.40
		0.455–0.793	1544–1696	CHS [13]	18	67	2.02
	B_l/A_0	0.295–0.435	1484–1536	Tripp [1]	15	60	1.02
		0.455–0.793	1544–1696	CHS [13]	18	65	0.79
				overall		2726	1.16
				with approximately 110 parameters			
(c) $\Lambda\pi$							
$\Lambda\pi^0$	$A_0, A_l/A_0$	0.245–0.445	1469–1540	Mast [1]	21	105	1.38
	$d\sigma/d\Omega$	0.455–0.853	1544–1723	CHS [13]	21	332	1.08
	$d\sigma/d\Omega$	0.862–0.936	1729–1764	Ch-LBL [14]	6	212	1.10
	$d\sigma/d\Omega$	0.960–1.355	1775–1957	RL-IC [2]	11	206	1.24
	$A_0, A_l/A_0$	1.368–1.843	1963–2169	CHM [15] [c]	13	104	1.42
				total	72	959	1.19
	B_l/A_0	0.245–0.445	1469–1540	Mast [1]	21	84	1.13
		0.455–0.853	1544–1723	CHS [13]	20	77	1.36
		0.862–0.936	1729–1764	Ch-LBL [14]	6	36	1.18
		0.960–1.355	1775–1957	RL-IC [2]	11	77	1.66
		1.368–1.843	1963–2169	CHM [15] [c]	13	91	1.21
				total	71	365	1.31
				overall		1324	1.22
				with approximately 64 parameters			

a) Includes one momentum from CRS [11].
b) Errors as discussed in the text; in the case of $\mathrm{Re}(f(0))/\mathrm{Im}(f(0))$ the χ^2 corresponds to an average χ^2 of 1.39 to the data at the five momenta at which the measurements were made.
c) Includes four momenta from CRS [11].

(d) Legendre shape coefficients A_l/A_0 for $K^-p \to \Sigma^0\pi^0$ at 33 momenta between 0.295 and 0.793 GeV/c.

(e) Associated Legendre coefficients, B_l/A_0 for $K^-p \to \Sigma^0\pi^0$ at the same momenta as (d).

(f) Cross sections and angular distributions for $K^0_L p \to \Sigma^0\pi^+$ at 11 momenta between 0.320 and 0.790 GeV/c [7].

(g) B_l/A_0 coefficients for $K^0_L p \to \Sigma^0\pi^+$ at the same momenta as (f).

2.3. The $\Lambda\pi$ channel

(a) Cross sections and angular distributions for $K^-p \to \Lambda\pi$ at 70 momenta between 0.245 and 1.843 GeV/c.

(b) B_l/A_0 coefficients for $K^-p \to \Lambda\pi$ at the same momenta. In the initial stages of fitting Legendre shape coefficients were used in all cases, but in the final fits the angular distributions listed above were fitted directly.

Table 1 summarises the data fitted, giving the experiments used for each of the classes listed above.

3. The parametrisation

In a reaction of the type $0^-\frac{1}{2}^+ \to 0^-\frac{1}{2}^+$ in which the target baryon is unpolarised, the differential cross section and polarisation are related to the partial waves by the following formalism:

$$\frac{d\sigma}{d\Omega} = \frac{k'}{k}\left[|f|^2 + |g|^2\right], \qquad P\frac{d\sigma}{d\Omega} = \frac{2k'}{k}\,\hat{n}\,\mathrm{Im}(fg^*),$$

where k and k' are the incoming and outgoing c.m. momenta and $\hat{n}$ is the normal to the production plane,

$$\hat{n} = \frac{k \times k'}{|k \times k'|}.$$

The amplitudes f and g are the usual non-flip and spin-flip amplitudes related to the partial waves by the expansions

$$f = \frac{1}{\sqrt{kk'}} \sum_l \left[(l+1)T_l^+ + lT_l^-\right]P_l(\cos\theta),$$

$$g = \frac{1}{\sqrt{kk'}} \sum_l \left[T_l^+ - T_l^-\right]P_l^1(\cos\theta),$$

where θ is the c.m. scattering angle, $P_l^1 = \sin\theta\ \mathrm{d}P_l(\cos\theta)/\mathrm{d}(\cos\theta)$, and P_l is the lth order Legendre polynomial;

$$T_{l^{\pm}} = c_0 T^0_{l^{\pm}} + c_1 T^1_{l^{\pm}} ,$$

where $T^I_{l^{\pm}}$ are the pure I-spin partial wave amplitudes with $J = l \pm \frac{1}{2}$, and c_I are the appropriate I-spin Clebsch-Gordan coefficients for a given reaction.

The pure I-spin partial wave amplitudes have been parametrised as

$$T = T_B + T_R ,$$

where T_B is the background term and T_R is a sum of non-relativistic Breit-Wigner resonances of the form

$$\frac{t}{\epsilon - i} e^{i\phi} ,$$

where t is the resonance amplitude and $\epsilon = (2/\Gamma(E))(E_R - E)$. The energy dependent width Γ is of the form

$$\Gamma(E) = \Gamma(E_R) \frac{k v_l(kr)}{k_R v_l(k_R r)} ,$$

where v_l is the Blatt and Weisskopf angular momentum barrier [8] for orbital angular momentum l. The radius of interaction, r, is taken to be 1 fm. In these formulae E is the c.m. energy and E_R and k_R are the values of E and k at the resonance energy. For the inelastic channels t also has a weak energy dependence,

$$t = \sqrt{XX'} = \sqrt{\frac{\Gamma_e \Gamma_i}{\Gamma^2}} ,$$

Γ_e and Γ_i being the partial widths of the elastic and the specific inelastic channel. The elastic partial width Γ_e has the same energy dependence as the total width but for Γ_i, k and k_R in the formula correspond to the c.m. momenta of the outgoing particles. It should be pointed out that the specific form assumed for the energy dependence of the width does not affect the results significantly. The resonance phase ϕ is fixed to zero for a dominant resonance in each energy region. (See table 2.)

The background term has the form

$$T_B = \sqrt{B_l B_{l'}}\, R(E) e^{i\theta(E)} ,$$

where

$$R(E) = \sum_{m=0}^{M} a_m P_m(E') , \qquad \theta(E) = \sum_{n=0}^{N} b_n P_n(E') ,$$

Table 2
Y^* parameters from best single channel fits

Wave	$\bar{K}N$				$\Sigma\pi$				$\Lambda\pi$			
	M (MeV)	Γ (MeV)	t	ϕ (rad)	M (MeV)	Γ (MeV)	t	ϕ (rad)	M (MeV)	Γ (MeV)	t	ϕ (rad)
S01	1670	45	0.17	(π)	1670	45	−0.35	−0.85				
S01	1823	230	0.39	0.77								
S11	1768	60	0.14	(0.0)					1710	68	−0.09	−0.02
S11	1955	200	0.49	1.18	1960	101	0.18	1.38	(1955)	145	0.06	−1.54
P01	1567	117	0.24	1.03	1584	191	−0.17	−0.67				
P01	1856	144	0.22	−0.94	1846	180	−0.20	0.96				
P11	1738	72	0.14	1.72	1676	117	−0.16	(0.0)				
P03	1900	72	0.18	1.07	1887	76	−0.09	−1.33				
D03	1519	15.4	0.47	[0.0]	1519	15.2	0.46	[0.0]				
D03	1692	55	0.23	[0.0]	1688	60	−0.26	−0.31				
D13	(1670)	(50)	0.09	[0.0]	1673	54	0.21	[0.0]	1665	45	0.09	0.57
D13					1901	390	−0.09	0.65	1986	173	−0.06	0.88
D05	(1825)	(90)	0.04	[0.0]	1825	94	−0.17	[0.0]				
D15	1774	136	0.42	[0.0]	1768	116	0.13	[0.0]	1777	124	−0.29	[0.0]
F05	1822	81	0.57	[0.0]	(1822)	(80)	−0.29	[0.0]				
F05	2045	197	0.08	−0.23	2130	243	0.12	−0.24				
F15	(1915)	(130)	0.05	−0.61	1914	128	−0.18	[0.0]	(1915)	121	−0.09	0.58
F17	2041	177	0.22	[0.0]	2050	210	−0.17	[0.0]	2037	179	0.19	[0.0]
G07	2110	250	0.30	[0.0]	(2116)	(230)	0.10	−0.51				
G09	1808	27	0.04	(0.0)								

Parameters M or Γ given in parentheses have been fixed from another channel (see text). The resonance amplitude (t) and phase ϕ are as defined in sect. 3. Note that t is defined positive for the $\bar{K}N$ channel, but in the other channels the sign of t must also be taken into account. A phase [0.0] indicates that the phase was fixed to zero throughout. A phase that stayed close to 0 or π was fixed to that value and is indicated in parentheses. For S01 (1670) the mass and width were kept at the same values in $\bar{K}N$ and $\Sigma\pi$.

$$E' = \frac{2E - E_{\max} - E_{\min}}{E_{\max} - E_{\min}},$$

such that E' equals +1 and −1 at energies $E_{\max}$ and $E_{\min}$ just above the upper end and below the lower end of the energy range fitted, and P_L are Legendre polynomials. The background parameters a_m and b_n are determined by fitting.

The angular momentum barrier factor B_l permits the smooth introduction of higher waves. For waves with $J \leqslant \frac{3}{2}$ this was set to unity. For the higher waves the form $B_l = (k/E)v_l(kr)$ was used in the $\Sigma\pi$ and $\Lambda\pi$ channels. In the $\bar{K}N$ channel where the effects of the high waves at low energies may be more important, the more flexible form $B_l = k^{2l+1}/(k^{2l+1} + k_0^{2l+1})$ was used, where k_0 is a constant determined by fitting.

The parameters of the resonance and background amplitudes have been determined by χ^2 fitting to the experimental data as described below, using the programme APPLE [9]. This analysis is not sensitive to structures with widths $\lesssim 20$ MeV since above 1540 MeV the energy spacing of the data used varies between 10 and 20 MeV c.m. (see table 1).

4. The fits

Initial partial wave solutions were developed for each channel over the energy range 1480–2170 MeV (referred to below as "the long range"), starting from the established resonances (as listed in table 3) and simple backgrounds ($N = M = 1$) in each wave. More complicated backgrounds were tried at later stages of the fitting. The initial solutions were refined by introducing additional resonance structure in regions where the fits were poor, or in waves where the background amplitude described an anticlockwise loop suggesting a resonance. A resonance was retained in the solution as a "probable" state if it satisfied the following criteria:

(a) the χ^2 to the data was significantly improved (reduction $\gtrsim 20$) in the region of that resonance;

(b) the resonance loop was clear on the Argand diagram and the speed variation of that amplitude showed a clear peak;

(c) the same improvement could not be obtained by introducing structure in other waves, or by using different backgrounds.

If the resonance only represented an alternative parametrisation of the wave that led to a simpler and smaller background, but did not give a significant improvement in χ^2, we term that state as "possible".

The parameters of the established resonances were investigated in each channel at several stages of the fitting, and subsequently fixed at consistent values in all channels. The final values decided are those in table 3. Specific problems with these parameters in any given channel are discussed below.

Table 3
Resonance parameters from the final solutions with consistent resonances (see text for discussion of errors)

Wave	M (MeV)	Γ (MeV)	$t_{\bar{K}N}$	$t_{\Sigma\pi}$	$t_{\Lambda\pi}$	Comment
S01	1670 ± 5	45 ± 10	0.20 ± 0.03	−0.31 ± 0.03		established
S01	1825 ± 20	230 ± 20	0.37 ± 0.05	−0.08 ± 0.05		possible
S11	1770 ± 15	60 ± 10	0.15 ± 0.03	−0.09 ± 0.05	(±)0.04 ± 0.03	probable
S11	1955 ± 15	170 ± 40	0.44 ± 0.05	0.20 ± 0.04	(±)0.08 ± 0.03	probable
P01	1573 ± 25	147 ± 50	0.24 ± 0.04	−0.16 ± 0.04		probable
P01	1853 ± 20	166 ± 20	0.21 ± 0.04	−0.24 ± 0.04		probable
P11	1738 ± 10	72 ± 10	0.14 ± 0.04			possible
P11	1676 ± 15	120 ± 20		−0.16 ± 0.03		probable
P03	1900 ± 5	72 ± 10	0.18 ± 0.02	−0.09 ± 0.03		now estab.
D03	1519 ± 1	15 ± 0.5	0.47 ± 0.01	0.46 ± 0.01		established
D03	1690 ± 5	60 ± 5	0.24 ± 0.03	−0.25 ± 0.03		established
D13	1670 ± 5	50 ± 5	0.08 ± 0.03	0.21 ± 0.02	0.10 ± 0.02	established
D13	1920 ± 50	300 ± 80		−0.08 ± 0.04	−0.06 ± 0.03	possible
D05	1825 ± 10	94 ± 10	0.04 ± 0.03	−0.17 ± 0.03		established
D15	1774 ± 5	130 ± 10	0.41 ± 0.03	0.13 ± 0.02	−0.28 ± 0.03	established
F05	1822 ± 2	81 ± 5	0.57 ± 0.02	−0.28 ± 0.03		established
F05	2100 ± 50	200 ± 50	0.07 ± 0.03	0.10 ± 0.03		possible
F15	1920 ± 10	130 ± 10	0.05 ± 0.03	−0.19 ± 0.03	−0.09 ± 0.03	established
F17	2040 ± 5	190 ± 10	0.24 ± 0.02	−0.15 ± 0.03	0.18 ± 0.02	established
G07	2110 ± 10	250 ± 30	0.30 ± 0.03	0.12 ± 0.04		established
G09	1808 ± 5	27 ± 5	0.04 ± 0.01			see text

In the $\bar{K}N$ and $\Sigma\pi$ channels where more data are available than in $\Lambda\pi$, the approach described above was also applied to fits over three shorter overlapping ranges so that the effects of new resonances could be examined in more detail. With a higher ratio of the number of free parameters to the number of data points in these short range solutions the fits to the data were considerably better than in the long range solutions. The information from these fits was used in the full range solutions.

The fitting of each of the three channels is described in the next three sections. The χ^2 contributions for each channel are given in table 1 and the resonance parameters for these solutions in table 2. The waves are described in sect. 5.

4.1. The $\bar{K}N$ solutions

Using the approach described above, solutions were developed for the long range and for three shorter overlapping regions: 1480 to 1740 MeV, 1700 to 1970 MeV and 1930 to 2170 MeV. The current long range solution was used to provide the starting values of the parameters for the short range fits. Additional information obtained from a short range solution was input to a new long range solution. The final long range solution was developed using information from all three short range fits. At this stage, to avoid the well known problems of correlations between the A_l/A_0 coefficients the fits were made directly to angular distributions (except in the case of the data of ref. [1] where the coefficients were retained since angular distributions were not available). The final solution has a χ^2 of 4010 for 3542 data points or a χ^2 of 1.18 per degree of freedom.

4.2. The $\Sigma\pi$ solutions

Solutions were developed over the long range and over three shorter ranges 1480 to 1780 MeV, 1700 to 1970 MeV and 1780 to 2170 MeV, in a similar manner to that described for the $\bar{K}N$ solutions. Using $K^0_L p \to \Sigma^0\pi^+$ and $K^- p \to \Sigma^0\pi^0$ data in addition to the $K^- p \to \Sigma^\pm\pi^\mp$ data in the region 1500 to 1700 MeV provided useful constraints to separate the $I = 0$ and $I = 1$ effects. The $\Sigma^0\pi^+$ angular distributions were particularly useful in obtaining stable values for the masses and widths of the established resonances D13(1670), D03(1690) and S01(1670), and also in showing clearly the P11(1680) state. There were problems fitting the $\Sigma^0\pi^0$ cross section above 1550 MeV. Since there are serious discrepancies between the data from different experiments in the region 1550 to 1700 MeV, these data were not included in the final fits. In the region of 1820 MeV the fits consistently predict $\Sigma^0\pi^0$ cross sections significantly higher than the measured values. Attempts to fit this worsen the $\Sigma^+\pi^-$ cross-section data in that region. Since no angular distribution data are available for $\Sigma^0\pi^0$ above 1700 MeV, the cross section was included in the final fits only as a general guide with the errors increased by a factor of three over the published values [2]. At higher energies, (above about 1850 MeV), where no pure I-spin data were available, it was found that the $I = 1$ $\bar{K}N \to \Sigma\pi$ predictions were very sen-

sitive to small changes in the parameters of the solution, although such changes left the fits to the $K^-p \to \Sigma^{\pm}\pi^{\mp}$ essentially unchanged.

As in $\bar{K}N$ the final fits were made directly to the angular distributions where available. Polarisation information was fitted as B_l/A_0 throughout but the fits were checked directly against the polarisation distributions. The final solution has a χ^2 of 3075 for 2726 data points or a χ^2 of 1.18 per degree of freedom.

4.3. The $\Lambda\pi$ solutions

Solutions were developed over the long range, using the approach described for the other channels. A short range solution was also developed over the range 1700 to 1970 MeV. In the final stages the angular distributions between 0.455 and 1.355 GeV/c were fitted directly, but above and below this range Legendre coefficients were fitted. The polarisation information was fitted in terms of B_l/A_0 over the whole range. Fits to the cross section give a high χ^2 (~2.5/data point) due to a scatter of the points rather than any systematic problem. It is assumed that this reflects the difficulty in extracting this cross section from the other $K^-p \to \Lambda$ + neutrals channels. For this reason the solutions were not modified to fix up these cross-section effects unless there were problems in the corresponding angular and polarisation distributions. For example, the fit to a dip in the cross section at about 1950 MeV is improved when a narrow P11 resonance is introduced, but this is not considered to be sufficient evidence for such a state. The final solution had a χ^2 of 1617 for 1324 data points corresponding to a χ^2 of 1.28 per degree of freedom.

4.4. Final solutions over full range (1480–2170 MeV) with consistent resonance parameters

In the solutions discussed above, except in the cases noted in sect. 5, the parameters of the states were free to search for the best value in each channel, and new resonances were included only if they were indicated in that channel. As a final stage resonances found in one channel were searched for in the other channels, and attempts were made to find solutions over the full range with consistent parameters for the corresponding states in each channel. The parameter values were chosen as a weighted average between the three channels depending on the relative coupling of the state and the stability of the parameters in each channel. The masses and widths were fixed at these values, and the background parameters, resonance couplings and phases varied to obtain the best fits. Where necessary the relative weightings were adjusted in order to find the set of parameters giving the minimum total χ^2. In the $\bar{K}N$ channel the χ^2 increased by 85 over the value obtained for the fits described above, giving a χ^2 per degree of freedom of 1.20. Similarly in the $\Lambda\pi$ channel the χ^2 increased by 49 giving a χ^2 of 1.31 per degree of freedom. In the $\Sigma\pi$ solution there was no significant change in the χ^2.

The final set of resonance parameters are given in table 3. The errors quoted are

Table 4
Partial-wave amplitudes from final consistent resonances solutions, given as Real part, Imaginary part every 10 MeV c.m. energy
(a) $\bar{K}N \to \bar{K}N$ $I = 0$

ENERGY	S01	P01	P03	D03	D05	F05	F07	G07	G09	H09
1480	0.03 0.73	0.07 0.0	0.02 0.0	0.03 0.0	0.0 0.0	0.0 0.0	0.0 0.0	0.0 0.0	0.0 0.0	0.0 0.0
1490	0.03 0.73	0.10 0.0	0.03 0.0	0.05 0.0	0.0 0.0	0.0 0.0	0.0 0.0	0.0 0.0	0.0 0.0	0.0 0.0
1500	0.04 0.74	0.13 0.02	0.05 0.0	0.11 0.02	0.0 0.0	0.0 0.0	0.0 0.0	0.0 0.0	0.0 0.0	0.0 0.0
1510	0.04 0.74	0.16 0.04	0.06 0.0	0.22 0.14	0 0 0.0	0.0 0.0	0.0 0.0	0.0 0.0	0.0 0.0	0.0 0.0
1520	0.04 0.75	0.19 0.06	0.08 0.01	-.05 0.45	0.0 0.0	0.0 0.0	0.0 0.0	0.0 0.0	0.0 0.0	0.0 0.0
1530	0.04 0.75	0.22 0.10	0.09 0.01	-.22 0.19	0.0 0.0	0.0 0.0	0.0 0.0	0.0 0.0	0.0 0.0	0.0 0.0
1540	0.04 0.75	0.24 0.14	0.11 0.02	-.19 0.09	0.0 0.0	0.0 0.0	0.0 0.0	0.0 0.0	0.0 0.0	0.0 0.0
1550	0.04 0.76	0.25 0.19	0.12 0.02	-.16 0.05	0.0 0.0	0.0 0.0	0.0 0.0	0.0 0.0	0.0 0.0	0.0 0.0
1560	0.04 0.76	0.25 0.23	0.13 0.03	-.14 0.04	0.0 0.0	0.0 0.0	0.0 0.0	0.0 0.0	0.0 0.0	0.0 0.0
1570	0.04 0.77	0.24 0.29	0.15 0.03	-.12 0.02	0.0 0.0	0.0 0.0	0.0 0.0	0.0 0.0	0.0 0.0	0.0 0.0
1580	0.04 0.77	0.22 0.31	0.16 0.04	-.10 0.32	0.0 0.0	0.01 0.0	0.0 0.0	0.0 0.0	0.0 0.0	0.0 0.0
1590	0.03 0.78	0.20 0.33	0.17 0.04	-.09 0.01	0.0 0.0	0.01 0.0	0.0 0.0	0.0 0.0	0.0 0.0	0.0 0.0
1600	0.03 0.78	0.19 0.35	0.19 0.05	-.08 0.0	0.0 0.0	0.02 0.0	0.0 0.0	0.0 0.0	0.0 0.0	0.0 0.0
1610	0.02 0.78	0.16 0.37	0.19 0.06	-.06 0.0	0.0 0.0	0.02 0.0	0.0 0.0	0.0 0.0	0.0 0.0	0.0 0.0
1620	0.01 0.79	0.15 0.38	0.21 0.07	-.05 0.0	0.0 0.0	0.02 0.0	0.0 0.0	0.0 0.0	0.0 0.0	0.0 0.0
1630	0.0 0.77	0.14 0.38	0.22 0.07	-.03 0.02	0.01 0.0	0.03 0.0	0.0 0.0	0.0 0.0	0.0 0.0	0.0 0.0
1640	0.0 0.75	0.13 0.39	0.23 0.08	0.0 0.03	0.02 0.0	0.04 0.0	0.0 0.0	0.0 0.0	0.0 0.0	0.0 0.0
1650	0.0 0.71	0.12 0.40	0.24 0.09	0.01 0.05	0.02 0.0	0.04 0.0	0.0 0.0	0.0 0.0	0.0 0.0	0.0 0.0
1660	0.03 0.67	0.11 0.40	0.25 0.10	0.03 0.08	0.02 0.0	0.05 0.0	0.0 0.0	0.0 0.0	0.0 0.0	0.0 0.0
1670	0.11 0.66	0.11 0.41	0.25 0.11	0.03 0.13	0.03 0.0	0.06 0.0	0.0 0.0	0.0 0.0	0.0 0.0	0.0 0.0
1680	0.17 0.72	0.11 0.42	0.26 0.12	0.0 0.19	0.03 0.0	0.07 0.0	0.0 0.0	0.0 0.0	0.0 0.0	0.0 0.0
1690	0.18 0.79	0.10 0.42	0.27 0.14	-.07 0.22	0.04 0.0	0.08 0.01	0.0 0.0	0.0 0.0	0.0 0.0	0.0 0.0
1700	0.17 0.83	0.10 0.43	0.28 0.15	-.14 0.19	0.04 0.0	0.10 0.01	0.0 0.0	0.0 0.0	0.0 0.0	0.0 0.0
1710	0.15 0.87	0.10 0.44	0.28 0.16	-.17 0.15	0.05 0.0	0.11 0.02	0.0 0.0	0.0 0.0	0.0 0.0	0.0 0.0
1720	0.13 0.90	0.10 0.45	0.29 0.17	-.17 0.11	0.05 0.01	0.13 0.03	0.0 0.0	0.0 0.0	0.0 0.0	0.0 0.0
1730	0.11 0.92	0.09 0.46	0.30 0.19	-.17 0.08	0.06 0.01	0.15 0.04	0.0 0.0	0.0 0.0	0.0 0.0	0.0 0.0
1740	0.08 0.94	0.09 0.47	0.30 0.20	-.16 0.06	0.07 0.02	0.18 0.05	0.0 0.0	0.0 0.0	0.0 0.0	0.0 0.0
1750	0.06 0.95	0.09 0.48	0.30 0.22	-.14 0.04	0.07 0.02	0.21 0.07	0.0 0.0	0.01 0.0	0.0 0.0	0.0 0.0
1760	0.03 0.97	0.08 0.49	0.31 0.23	-.13 0.04	0.08 0.03	0.24 0.11	0.0 0.0	0.01 0.0	0.0 0.0	0.0 0.0
1770	0.0 0.98	0.07 0.50	0.31 0.25	-.12 0.02	0.08 0.03	0.27 0.15	0.0 0.0	0.02 0.0	0.0 0.0	0.0 0.0
1780	-.03 0.98	0.06 0.51	0.31 0.26	-.11 0.02	0.09 0.04	0.30 0.22	0.0 0.0	0.02 0.0	0.01 0.0	0.0 0.0
1790	-.07 0.98	0.05 0.52	0.31 0.28	-.10 0.02	0.09 0.05	0.31 0.31	0.0 0.0	0.02 0.0	0.02 0.01	0.0 0.0
1800	-.10 0.97	0.04 0.53	0.31 0.30	-.09 0.02	0.09 0.06	0.28 0.42	0.0 0.0	0.02 0.0	0.02 0.03	0.0 0.0
1810	-.13 0.96	0.02 0.53	0.31 0.32	-.08 0.02	0.09 0.06	0.19 0.52	0.0 0.0	0.02 0.0	0.0 0.04	0.0 0.0
1820	-.16 0.94	0.0 0.53	0.31 0.34	-.07 0.02	0.09 0.07	0.06 0.57	0.0 0.0	0.03 0.0	-.01 0.02	0.0 0.0
1830	-.18 0.91	-.02 0.53	0.30 0.36	-.06 0.02	0.08 0.08	-.07 0.56	0.0 0.0	0.03 0.0	-.01 0.01	0.0 0.0
1840	-.20 0.89	-.03 0.52	0.30 0.38	-.05 0.02	0.08 0.09	-.16 0.50	0.0 0.0	0.03 0.0	-.01 0.0	0.0 0.0
1850	-.22 0.86	-.05 0.50	0.28 0.41	-.05 0.03	0.08 0.07	-.21 0.42	0.0 0.0	0.04 0.0	0.0 0.0	0.0 0.0
1860	-.23 0.83	-.05 0.49	0.26 0.44	-.04 0.03	0.08 0.07	-.23 0.36	0.0 0.0	0.04 0.0	0.0 0.0	0.0 0.0
1870	-.23 0.81	-.06 0.47	0.24 0.46	-.03 0.03	0.08 0.07	-.23 0.31	0.0 0.0	0.05 0.0	0.0 0.0	0.01 0.0
1880	-.23 0.78	-.05 0.45	0.20 0.48	-.03 0.04	0.08 0.07	-.23 0.27	0.0 0.0	0.05 0.0	0.0 0.0	0.01 0.0
1890	-.23 0.76	-.05 0.43	0.15 0.48	-.02 0.04	0.09 0.08	-.22 0.23	0.0 0.0	0.06 0.0	0.0 0.0	0.01 0.0
1900	-.23 0.73	-.04 0.42	0.11 0.46	-.02 0.05	0.09 0.08	-.21 0.21	0.0 0.0	0.06 0.01	0.0 0.0	0.01 0.0
1910	-.22 0.72	-.02 0.41	0.10 0.42	-.01 0.06	0.10 0.08	-.20 0.19	0.0 0.0	0.07 0.01	0.0 0.0	0.02 0.0
1920	-.21 0.70	-.01 0.41	0.10 0.40	0.0 0.06	0.10 0.08	-.19 0.18	0.0 0.0	0.08 0.02	0.0 0.0	0.02 0.0
1930	-.20 0.68	0.0 0.40	0.11 0.38	0.0 0.07	0.10 0.09	-.18 0.16	0.01 0.0	0.09 0.02	0.0 0.0	0.02 0.0
1940	-.19 0.67	0.02 0.40	0.12 0.38	0.0 0.09	0.10 0.09	-.17 0.16	0.01 0.0	0.09 0.03	0.0 0.0	0.02 0.0
1950	-.19 0.66	0.03 0.40	0.13 0.39	0.0 0.08	0.11 0.10	-.16 0.15	0.01 0.0	0.10 0.03	0.0 0.0	0.02 0.0
1960	-.18 0.65	0.04 0.40	0.13 0.40	0.0 0.09	0.11 0.10	-.15 0.15	0.01 0.0	0.11 0.04	0.0 0.0	0.02 0.0
1970	-.17 0.64	0.05 0.40	0.13 0.41	0.0 0.10	0.11 0.11	-.14 0.14	0.02 0.01	0.12 0.05	0.0 0.0	0.03 0.0
1980	-.16 0.63	0.06 0.41	0.13 0.42	0.0 0.11	0.11 0.11	-.13 0.14	0.02 0.01	0.13 0.06	0.0 0.0	0.03 0.0
1990	-.15 0.62	0.07 0.41	0.12 0.43	0.0 0.11	0.12 0.12	-.13 0.14	0.02 0.01	0.13 0.07	0.01 0.0	0.03 0.0
2000	-.14 0.62	0.08 0.42	0.12 0.44	0.0 0.12	0.12 0.12	-.12 0.14	0.02 0.02	0.14 0.09	0.01 0.0	0.03 0.0
2010	-.13 0.61	0.09 0.42	0.11 0.46	0.0 0.13	0.12 0.13	-.12 0.14	0.02 0.02	0.15 0.11	0.01 0.0	0.03 0.0
2020	-.13 0.61	0.10 0.43	0.10 0.47	0.0 0.14	0.12 0.13	-.12 0.14	0.02 0.02	0.15 0.13	0.02 0.01	0.03 0.0
2030	-.12 0.60	0.10 0.43	0.08 0.47	0.0 0.15	0.12 0.14	-.12 0.14	0.03 0.03	0.14 0.15	0.02 0.01	0.04 0.0
2040	-.11 0.60	0.11 0.44	0.07 0.48	-.01 0.15	0.12 0.15	-.12 0.14	0.03 0.03	0.14 0.17	0.02 0.01	0.04 0.0
2050	-.11 0.60	0.12 0.45	0.06 0.49	-.01 0.16	0.12 0.15	-.12 0.15	0.03 0.03	0.13 0.19	0.02 0.01	0.04 0.0
2060	-.10 0.59	0.12 0.45	0.04 0.50	-.02 0.17	0.12 0.16	-.12 0.15	0.03 0.04	0.11 0.20	0.02 0.01	0.04 0.0
2070	-.09 0.59	0.13 0.46	0.03 0.50	-.02 0.18	0.12 0.16	-.13 0.14	0.03 0.04	0.10 0.22	0.03 0.02	0.04 0.0
2080	-.09 0.59	0.11 0.47	0.0 0.51	-.03 0.19	0.12 0.17	-.13 0.14	0.03 0.05	0.08 0.23	0.03 0.02	0.04 0.0
2090	-.08 0.59	0.14 0.48	0.0 0.51	-.04 0.19	0.12 0.18	-.14 0.14	0.03 0.05	0.05 0.24	0.03 0.02	0.04 0.0
2100	-.08 0.58	0.14 0.48	-.02 0.52	-.04 0.20	0.12 0.18	-.14 0.13	0.04 0.06	0.03 0.24	0.03 0.02	0.04 0.0
2110	-.07 0.58	0.14 0.49	-.04 0.52	-.05 0.20	0.12 0.19	-.15 0.13	0.04 0.07	0.0 0.24	0.04 0.02	0.04 0.0
2120	-.07 0.59	0.15 0.50	-.06 0.52	-.06 0.21	0.12 0.20	-.15 0.12	0.04 0.07	-.01 0.23	0.04 0.02	0.04 0.0
2130	-.07 0.58	0.15 0.51	-.08 0.52	-.07 0.21	0.12 0.20	-.15 0.11	0.04 0.08	-.03 0.22	0.04 0.02	0.03 0.0
2140	-.06 0.59	0.15 0.51	-.10 0.52	-.07 0.22	0.12 0.21	-.16 0.10	0.04 0.09	-.05 0.21	0.04 0.03	0.03 0.0
2150	-.06 0.57	0.15 0.52	-.12 0.52	-.08 0.22	0.12 0.22	-.16 0.10	0.03 0.09	-.06 0.19	0.05 0.03	0.03 0.0
2160	-.05 0.57	0.15 0.53	-.13 0.52	-.09 0.23	0.11 0.22	-.16 0.09	0.03 0.10	-.07 0.18	0.05 0.03	0.02 0.0
2170	-.05 0.57	0.16 0.54	-.15 0.51	-.10 0.23	0.11 0.23	-.16 0.08	0.03 0.11	-.07 0.16	0.05 0.03	0.02 0.0

Table 4 (continued)
(b) $\bar{K}N \to \bar{K}N$ $I = 1$

ENERGY	S11	P11	P13	D13	D15	F15	F17	G17	G19	H19
1480	0.20 0.33	0.04 0.0	-.05 0.03	-.02 0.0	0.0 0.0	0.0 0.0	0.0 0.0	0.0 0.0	0.0 0.0	0.0 0.0
1490	0.20 0.33	0.04 0.0	-.05 0.03	-.01 0.0	0.0 0.0	0.0 0.0	0.0 0.0	0.0 0.0	0.0 0.0	0.0 0.0
1500	0.20 0.34	0.05 0.0	-.04 0.02	0.0 0.0	0.0 0.0	0.0 0.0	0.0 0.0	0.0 0.0	0.0 0.0	0.0 0.0
1510	0.20 0.34	0.05 0.0	-.04 0.02	0.0 0.0	0.01 0.0	0.0 0.0	0.0 0.0	0.0 0.0	0.0 0.0	0.0 0.0
1520	0.20 0.35	0.06 0.01	-.03 0.01	0.0 0.0	0.01 0.0	0.0 0.0	0.0 0.0	0.0 0.0	0.0 0.0	0.0 0.0
1530	0.20 0.35	0.06 0.02	-.03 0.0	0.0 0.0	0.02 0.0	0.0 0.0	0.0 0.0	0.0 0.0	0.0 0.0	0.0 0.0
1540	0.20 0.36	0.06 0.02	-.03 0.0	0.0 0.0	0.02 0.0	0.0 0.0	0.0 0.0	0.0 0.0	0.0 0.0	0.0 0.0
1550	0.20 0.36	0.07 0.03	-.02 0.0	0.0 0.0	0.03 0.0	0.0 0.0	0.0 0.0	0.0 0.0	0.0 0.0	0.0 0.0
1560	0.20 0.37	0.07 0.03	-.01 0.0	0.01 0.0	0.03 0.0	0.0 0.0	0.0 0.0	0.0 0.0	0.0 0.0	0.0 0.0
1570	0.20 0.37	0.07 0.04	0.0 0.0	0.02 0.0	0.04 0.0	0.0 0.0	0.0 0.0	0.0 0.0	0.0 0.0	0.0 0.0
1580	0.20 0.38	0.08 0.04	0.0 0.0	0.02 0.0	0.05 0.0	0.0 0.0	0.0 0.0	0.0 0.0	0.0 0.0	0.0 0.0
1590	0.20 0.38	0.08 0.05	0.0 0.0	0.03 0.0	0.05 0.0	0.0 0.0	0.0 0.0	0.0 0.0	0.0 0.0	0.0 0.0
1600	0.20 0.39	0.08 0.06	0.0 0.0	0.03 0.01	0.06 0.0	0.0 0.0	0.0 0.0	0.0 0.0	0.0 0.0	0.0 0.0
1610	0.20 0.39	0.08 0.06	0.01 0.0	0.04 0.01	0.07 0.01	0.0 0.0	0.0 0.0	0.0 0.0	0.0 0.0	0.0 0.0
1620	0.20 0.40	0.08 0.07	0.02 0.0	0.04 0.02	0.08 0.02	0.0 0.0	0.0 0.0	0.0 0.0	0.0 0.0	0.0 0.0
1630	0.20 0.41	0.08 0.08	0.02 0.0	0.05 0.03	0.09 0.02	0.0 0.0	0.0 0.0	0.0 0.0	0.0 0.0	0.0 0.0
1640	0.21 0.41	0.08 0.09	0.03 0.0	0.06 0.04	0.11 0.03	0.0 0.0	0.0 0.0	0.0 0.0	0.0 0.0	0.0 0.0
1650	0.21 0.42	0.08 0.10	0.03 0.01	0.06 0.06	0.12 0.04	0.0 0.0	0.01 0.0	0.0 0.0	0.0 0.0	0.0 0.0
1660	0.21 0.43	0.07 0.11	0.04 0.02	0.05 0.09	0.13 0.05	0.0 0.0	0.01 0.0	0.0 0.0	0.0 0.0	0.0 0.0
1670	0.21 0.43	0.07 0.12	0.04 0.02	0.02 0.11	0.15 0.06	0.0 0.0	0.02 0.0	0.0 0.0	0.0 0.0	0.0 0.0
1680	0.21 0.44	0.06 0.12	0.05 0.02	0.0 0.10	0.17 0.08	0.0 0.0	0.02 0.0	0.0 0.0	0.0 0.0	0.0 0.0
1690	0.21 0.45	0.05 0.13	0.05 0.03	-.01 0.08	0.18 0.10	0.0 0.0	0.02 0.0	0.0 0.0	0.0 0.0	0.0 0.0
1700	0.22 0.47	0.03 0.14	0.05 0.03	-.01 0.07	0.20 0.13	0.0 0.0	0.02 0.0	0.0 0.0	0.0 0.0	0.0 0.0
1710	0.22 0.48	0.0 0.14	0.06 0.04	-.01 0.07	0.21 0.17	0.0 0.0	0.03 0.0	0.0 0.0	0.0 0.0	0.0 0.0
1720	0.22 0.50	-.02 0.13	0.06 0.05	0.0 0.06	0.21 0.21	0.0 0.0	0.03 0.0	0.0 0.0	0.0 0.0	0.0 0.0
1730	0.23 0.52	-.04 0.10	0.06 0.05	0.0 0.06	0.21 0.26	0.0 0.0	0.03 0.0	0.0 0.0	0.0 0.0	0.0 0.0
1740	0.23 0.55	-.04 0.07	0.06 0.06	0.0 0.06	0.19 0.31	0.01 0.0	0.04 0.0	0.0 0.0	0.0 0.0	0.0 0.0
1750	0.21 0.59	-.02 0.04	0.06 0.06	0.0 0.06	0.15 0.36	0.01 0.0	0.04 0.0	0.0 0.0	0.0 0.0	0.0 0.0
1760	0.18 0.63	0.0 0.03	0.07 0.07	0.0 0.06	0.10 0.39	0.02 0.0	0.04 0.0	0.0 0.0	0.0 0.0	0.0 0.0
1770	0.13 0.65	0.02 0.03	0.07 0.08	0.0 0.06	0.04 0.41	0.02 0.0	0.05 0.0	0.0 0.0	0.0 0.0	0.0 0.0
1780	0.08 0.64	0.04 0.04	0.07 0.08	0.0 0.07	-.02 0.41	0.02 0.0	0.05 0.0	0.0 0.0	0.0 0.0	0.0 0.0
1790	0.06 0.63	0.05 0.05	0.07 0.09	0.0 0.07	-.07 0.39	0.02 0.0	0.06 0.0	0.0 0.0	0.0 0.0	0.0 0.0
1800	0.04 0.61	0.06 0.06	0.07 0.10	0.0 0.07	-.12 0.37	0.03 0.0	0.06 0.0	0.0 0.0	0.0 0.0	0.0 0.0
1810	0.04 0.60	0.06 0.07	0.07 0.10	0.0 0.07	-.14 0.33	0.03 0.0	0.07 0.01	0.0 0.0	0.0 0.0	0.0 0.0
1820	0.03 0.60	0.07 0.08	0.07 0.11	0.0 0.08	-.16 0.30	0.03 0.0	0.07 0.01	0.0 0.0	0.0 0.0	0.0 0.0
1830	0.02 0.61	0.07 0.09	0.07 0.12	0.0 0.08	-.17 0.27	0.04 0.0	0.08 0.01	0.0 0.0	0.0 0.0	0.0 0.0
1840	0.02 0.62	0.07 0.10	0.07 0.12	0.0 0.08	-.17 0.25	0.04 0.0	0.09 0.02	0.0 0.0	0.0 0.0	0.0 0.0
1850	0.0 0.63	0.06 0.10	0.07 0.13	0.0 0.08	-.17 0.22	0.05 0.0	0.09 0.02	0.0 0.0	0.0 0.0	0.0 0.0
1860	-.02 0.64	0.06 0.11	0.07 0.14	0.0 0.09	-.17 0.20	0.05 0.0	0.10 0.02	0.0 0.0	0.0 0.0	0.0 0.0
1870	-.04 0.65	0.06 0.11	0.06 0.14	0.0 0.09	-.17 0.19	0.05 0.0	0.11 0.03	0.0 0.0	0.0 0.0	0.0 0.0
1880	-.06 0.66	0.06 0.12	0.06 0.15	0.0 0.09	-.16 0.17	0.06 0.01	0.12 0.03	0.0 0.0	0.0 0.0	0.0 0.0
1890	-.09 0.66	0.06 0.13	0.06 0.16	0.0 0.09	-.15 0.16	0.06 0.02	0.12 0.04	0.0 0.0	0.0 0.0	0.0 0.0
1900	-.13 0.66	0.05 0.13	0.06 0.16	0.0 0.10	-.14 0.15	0.06 0.02	0.13 0.05	0.01 0.0	0.0 0.0	0.0 0.0
1910	-.17 0.66	0.05 0.13	0.06 0.17	0.0 0.10	-.14 0.14	0.05 0.03	0.14 0.05	0.01 0.0	0.0 0.0	0.0 0.0
1920	-.21 0.64	0.05 0.14	0.06 0.18	0.0 0.10	-.13 0.14	0.05 0.04	0.15 0.06	0.01 0.0	0.0 0.0	0.0 0.0
1930	-.25 0.62	0.04 0.14	0.05 0.18	0.0 0.10	-.12 0.13	0.04 0.04	0.16 0.08	0.01 0.0	0.0 0.0	0.0 0.0
1940	-.29 0.59	0.04 0.15	0.05 0.19	0.0 0.11	-.11 0.13	0.03 0.04	0.16 0.09	0.02 0.01	0.0 0.0	0.0 0.0
1950	-.32 0.54	0.03 0.15	0.05 0.19	0.01 0.11	-.10 0.13	0.02 0.04	0.17 0.10	0.02 0.01	0.0 0.0	0.0 0.0
1960	-.33 0.50	0.03 0.15	0.05 0.20	0.01 0.11	-.10 0.12	0.01 0.04	0.17 0.12	0.02 0.01	0.0 0.0	0.0 0.0
1970	-.34 0.45	0.03 0.15	0.05 0.21	0.01 0.11	-.09 0.12	0.0 0.04	0.18 0.14	0.02 0.02	0.0 0.0	0.0 0.0
1980	-.34 0.40	0.02 0.16	0.05 0.21	0.01 0.12	-.08 0.12	0.0 0.04	0.17 0.16	0.02 0.02	0.0 0.01	0.0 0.0
1990	-.32 0.36	0.02 0.16	0.04 0.22	0.02 0.12	-.07 0.12	-.01 0.04	0.17 0.18	0.02 0.02	0.0 0.01	0.0 0.0
2000	-.30 0.33	0.01 0.16	0.04 0.23	0.02 0.12	-.07 0.12	-.02 0.05	0.15 0.20	0.03 0.02	0.0 0.01	0.0 0.0
2010	-.28 0.30	0.01 0.16	0.04 0.23	0.02 0.12	-.06 0.12	-.02 0.05	0.14 0.22	0.03 0.02	0.0 0.01	0.0 0.0
2020	-.26 0.28	0.0 0.16	0.04 0.24	0.02 0.13	-.05 0.12	-.03 0.05	0.12 0.23	0.03 0.03	0.01 0.01	0.01 0.0
2030	-.23 0.26	0.0 0.16	0.04 0.24	0.03 0.13	-.05 0.13	-.01 0.06	0.10 0.24	0.03 0.03	0.01 0.01	0.01 0.0
2040	-.21 0.25	0.0 0.17	0.04 0.25	0.03 0.13	-.04 0.13	-.04 0.06	0.07 0.24	0.03 0.03	0.01 0.01	0.02 0.0
2050	-.19 0.25	0.0 0.17	0.04 0.25	0.03 0.13	-.03 0.13	-.04 0.07	0.05 0.24	0.04 0.04	0.01 0.01	0.02 0.0
2060	-.17 0.24	0.0 0.17	0.03 0.26	0.04 0.13	-.03 0.14	-.04 0.07	0.03 0.23	0.04 0.04	0.01 0.01	0.02 0.0
2070	-.15 0.24	-.01 0.17	0.03 0.27	0.04 0.13	-.02 0.14	-.04 0.08	0.01 0.22	0.04 0.04	0.01 0.01	0.02 0.0
2080	-.14 0.24	-.02 0.17	0.03 0.27	0.04 0.14	-.02 0.14	-.04 0.09	0.0 0.21	0.04 0.05	0.01 0.01	0.03 0.0
2090	-.13 0.24	-.02 0.17	0.03 0.28	0.05 0.14	-.01 0.15	-.04 0.10	-.01 0.20	0.05 0.05	0.01 0.01	0.03 0.0
2100	-.11 0.24	-.02 0.17	0.03 0.28	0.05 0.14	0.0 0.15	-.04 0.11	-.02 0.19	0.05 0.06	0.0 0.01	0.03 0.0
2110	-.10 0.25	-.03 0.17	0.03 0.29	0.06 0.14	0.0 0.16	-.04 0.12	-.03 0.17	0.05 0.06	0.0 0.01	0.04 0.0
2120	-.10 0.25	-.03 0.16	0.03 0.29	0.06 0.14	0.0 0.16	-.04 0.13	-.03 0.16	0.05 0.07	0.0 0.01	0.04 0.0
2130	-.09 0.25	-.04 0.16	0.03 0.30	0.07 0.14	0.0 0.17	-.03 0.14	-.04 0.15	0.06 0.07	0.0 0.0	0.05 0.0
2140	-.08 0.26	-.04 0.16	0.04 0.30	0.07 0.14	0.01 0.17	-.02 0.15	-.04 0.14	0.06 0.08	0.0 0.0	0.05 0.0
2150	-.07 0.26	-.04 0.16	0.04 0.31	0.08 0.14	0.02 0.18	-.02 0.16	-.04 0.13	0.06 0.09	0.0 0.0	0.06 0.0
2160	-.07 0.26	-.04 0.16	0.04 0.32	0.09 0.14	0.02 0.18	0.0 0.17	-.04 0.12	0.06 0.09	0.0 0.0	0.07 0.0
2170	-.06 0.27	-.05 0.16	0.04 0.32	0.09 0.13	0.02 0.19	0.0 0.18	-.04 0.11	0.07 0.10	0.0 0.0	0.08 0.0

Table 4 (continued)
(c) $\bar{K}N \to \Sigma\pi$ $I = 0$

ENERGY	S01	P01	P03	D03	D05	F05	F07	G07	G09	H09
1480	-.32 0.30	-.03 0.0	0.05 0.0	0.04 0.0	0.0 0.0	0.0 0.0	0.0 0.0	0.0 0.0	0.0 0.0	0.0 0.0
1490	-.30 0.31	-.05 -.01	0.05 0.0	0.07 0.0	0.0 0.0	0.0 0.0	0.0 0.0	0.0 0.0	0.0 0.0	0.0 0.0
1500	-.29 0.31	-.06 -.02	0.05 0.0	0.12 0.02	0.0 0.0	0.0 0.0	0.0 0.0	0.0 0.0	0.0 0.0	0.0 0.0
1510	-.28 0.32	-.08 -.03	0.05 0.0	0.23 0.15	0.0 0.0	0.0 0.0	0.0 0.0	0.0 0.0	0.0 0.0	0.0 0.0
1520	-.27 0.32	-.10 -.05	0.06 0.0	-.06 0.44	0.0 0.0	0.0 0.0	0.0 0.0	0.0 0.0	0.0 0.0	0.0 0.0
1530	-.26 0.32	-.12 -.07	0.06 0.0	-.22 0.18	0.0 0.0	0.0 0.0	0.0 0.0	0.0 0.0	0.0 0.0	0.0 0.0
1540	-.26 0.32	-.13 -.10	0.06 0.0	-.18 0.09	0.0 0.0	0.0 0.0	0.0 0.0	0.0 0.0	0.0 0.0	0.0 0.0
1550	-.25 0.33	-.13 -.13	0.06 0.0	-.15 0.06	0.0 0.0	0.0 0.0	0.0 0.0	0.0 0.0	0.0 0.0	0.0 0.0
1560	-.24 0.33	-.12 -.16	0.07 0.0	-.14 0.04	0.0 0.0	0.0 0.0	0.0 0.0	0.0 0.0	0.0 0.0	0.0 0.0
1570	-.23 0.33	-.11 -.19	0.07 0.01	-.13 0.03	0.0 0.0	0.0 0.0	0.0 0.0	0.0 0.0	0.0 0.0	0.0 0.0
1580	-.23 0.33	-.10 -.21	0.07 0.01	-.12 0.01	-.01 0.0	0.0 0.0	0.0 0.0	0.0 0.0	0.0 0.0	0.0 0.0
1590	-.23 0.33	-.08 -.22	0.07 0.02	-.12 0.02	-.01 0.0	0.0 0.0	0.0 0.0	0.0 0.0	0.0 0.0	0.0 0.0
1600	-.23 0.33	-.07 -.23	0.08 0.02	-.12 0.02	-.01 0.0	0.0 0.0	0.0 0.0	0.0 0.0	0.0 0.0	0.0 0.0
1610	-.23 0.33	-.05 -.24	0.08 0.02	-.13 0.01	-.02 0.0	0.0 0.0	0.0 0.0	0.0 0.0	0.0 0.0	0.0 0.0
1620	-.24 0.33	-.04 -.24	0.08 0.02	-.14 0.0	-.02 0.0	0.0 0.0	0.01 0.0	0.0 0.0	0.0 0.0	0.0 0.0
1630	-.26 0.32	-.03 -.25	0.08 0.02	-.15 0.0	-.02 0.0	-.01 0.0	0.01 0.0	0.0 0.0	0.0 0.0	0.0 0.0
1640	-.29 0.30	-.03 -.25	0.09 0.03	-.16 -.01	-.02 0.0	-.01 0.0	0.01 0.0	0.0 0.0	0.0 0.0	0.0 0.0
1650	-.33 0.26	-.02 -.25	0.09 0.03	-.18 -.03	-.02 0.0	-.02 0.0	0.01 0.0	0.0 0.0	0.0 0.0	0.0 0.0
1660	-.36 0.16	-.02 -.25	0.09 0.03	-.20 -.07	-.03 0.0	-.02 0.0	0.02 0.0	0.0 0.0	0.0 0.0	0.0 0.0
1670	-.11 0.01	-.01 -.26	0.09 0.03	-.20 -.12	-.01 0.0	-.02 0.0	0.02 0.0	0.0 0.0	0.0 0.0	0.0 0.0
1680	-.19 -.03	-.01 -.26	0.09 0.04	-.17 -.19	-.01 0.0	-.01 0.0	0.02 0.0	0.0 0.0	0.0 0.0	0.0 0.0
1690	-.09 -.01	0.0 -.27	0.10 0.04	-.09 -.24	-.04 0.0	-.01 0.0	0.02 0.0	0.0 0.0	0.0 0.0	0.0 0.0
1700	-.04 0.02	0.0 -.27	0.10 0.04	-.01 -.23	-.04 -.01	-.04 0.0	0.02 0.0	0.0 -.01	0.0 0.0	0.0 0.0
1710	-.02 0.05	0.0 -.27	0.10 0.05	0.04 -.19	-.05 -.01	-.04 -.01	0.02 0.0	0.0 -.01	0.0 0.0	0.0 0.0
1720	0.0 0.07	0.0 -.28	0.10 0.05	0.06 -.15	-.05 -.02	-.05 -.01	0.02 0.0	0.0 -.01	0.0 0.0	0.0 0.0
1730	0.0 0.08	0.0 -.29	0.10 0.05	0.07 -.12	-.06 -.02	-.06 -.02	0.03 0.0	0.0 -.01	0.0 0.0	0.0 0.0
1740	0.02 0.08	0.0 -.29	0.10 0.06	0.07 -.10	-.06 -.03	-.07 -.03	0.03 0.0	0.0 -.01	0.0 0.0	0.0 0.0
1750	0.02 0.08	0.01 -.30	0.10 0.06	0.07 -.08	-.07 -.04	-.08 -.04	0.03 0.0	-.01 -.01	0.0 0.0	0.0 0.0
1760	0.03 0.08	0.02 -.31	0.10 0.06	0.07 -.07	-.08 -.05	-.10 -.05	0.03 0.0	-.01 0.0	0.0 0.0	0.0 0.0
1770	0.04 0.07	0.03 -.32	0.10 0.07	0.07 -.05	-.08 -.06	-.11 -.07	0.03 0.0	-.01 0.0	0.0 0.0	0.0 0.0
1780	0.05 0.07	0.04 -.32	0.10 0.07	0.07 -.04	-.08 -.08	-.12 -.11	0.03 0.0	-.01 0.0	0.0 0.0	0.0 0.0
1790	0.05 0.06	0.05 -.33	0.10 0.08	0.07 -.04	-.08 -.10	-.12 -.15	0.01 0.0	-.02 0.0	0.0 0.0	0.0 0.0
1800	0.06 0.05	0.07 -.33	0.10 0.08	0.07 -.03	-.07 -.13	-.11 -.20	0.03 0.0	-.02 0.0	0.0 0.0	0.0 0.0
1810	0.07 0.05	0.09 -.33	0.10 0.09	0.07 -.02	-.05 -.15	-.06 -.25	0.03 0.0	-.01 0.0	0.0 0.0	0.0 0.0
1820	0.08 0.04	0.11 -.32	0.10 0.09	0.07 -.02	-.02 -.17	0.0 -.28	0.04 0.0	-.01 0.0	0.0 0.0	0.0 0.0
1830	0.09 0.03	0.13 -.31	0.10 0.10	0.07 -.01	0.02 -.17	0.07 -.27	0.04 0.0	-.01 0.01	0.0 0.0	0.0 0.0
1840	0.10 0.03	0.15 -.29	0.09 0.10	0.07 -.01	0.05 -.16	0.12 -.24	0.04 0.01	0.0 0.01	0.0 0.0	0.0 0.0
1850	0.11 0.03	0.17 -.26	0.08 0.10	0.07 0.0	0.07 -.14	0.14 -.20	0.04 0.01	0.0 0.02	0.0 0.0	0.0 0.0
1860	0.11 0.02	0.17 -.23	0.07 0.10	0.07 0.0	0.08 -.12	0.16 -.17	0.04 0.01	0.0 0.02	0.0 0.0	0.0 0.0
1870	0.12 0.02	0.18 -.21	0.06 0.10	0.07 0.0	0.08 -.10	0.16 -.14	0.04 0.01	0.0 0.02	0.0 0.0	0.0 0.0
1880	0.12 0.02	0.17 -.18	0.05 0.09	0.07 0.0	0.09 -.08	0.16 -.12	0.04 0.01	0.0 0.02	0.0 0.0	0.0 0.0
1890	0.12 0.02	0.16 -.15	0.05 0.08	0.07 0.0	0.08 -.07	0.16 -.11	0.04 0.02	0.0 0.02	0.0 0.0	0.0 0.0
1900	0.12 0.02	0.15 -.13	0.05 0.06	0.07 0.01	0.08 -.06	0.16 -.09	0.04 0.02	0.01 0.03	0.0 0.0	0.0 0.0
1910	0.12 0.01	0.14 -.11	0.07 0.04	0.07 0.02	0.08 -.05	0.16 -.08	0.04 0.02	0.02 0.03	0.0 0.0	0.0 0.0
1920	0.12 0.01	0.12 -.09	0.09 0.04	0.07 0.02	0.08 -.04	0.16 -.07	0.03 0.02	0.02 0.03	0.01 0.0	0.0 0.0
1930	0.12 0.0	0.11 -.08	0.11 0.05	0.07 0.02	0.07 -.04	0.16 -.06	0.03 0.02	0.03 0.03	0.01 0.0	0.0 0.0
1940	0.12 0.0	0.09 -.07	0.12 0.06	0.07 0.03	0.07 -.03	0.16 -.06	0.03 0.02	0.03 0.03	0.01 0.0	0.0 0.0
1950	0.12 0.0	0.08 -.06	0.11 0.07	0.07 0.03	0.07 -.03	0.16 -.05	0.03 0.02	0.04 0.03	0.01 0.0	0.0 0.0
1960	0.11 0.0	0.06 -.05	0.13 0.08	0.07 0.04	0.06 -.03	0.16 -.04	0.03 0.02	0.04 0.03	0.01 0.0	0.0 0.0
1970	0.11 0.0	0.05 -.04	0.14 0.08	0.07 0.04	0.06 -.03	0.16 -.04	0.03 0.02	0.05 0.03	0.01 0.0	0.0 0.0
1980	0.10 0.0	0.04 -.04	0.14 0.09	0.07 0.04	0.06 -.02	0.16 -.03	0.03 0.02	0.06 0.04	0.01 0.0	0.0 0.0
1990	0.10 -.01	0.03 -.03	0.14 0.10	0.07 0.05	0.06 -.02	0.16 -.02	0.03 0.02	0.06 0.04	0.01 0.0	0.0 0.0
2000	0.09 -.02	0.02 -.02	0.14 0.11	0.07 0.05	0.05 -.02	0.16 -.02	0.03 0.02	0.07 0.04	0.02 0.0	0.0 0.0
2010	0.09 -.02	0.01 -.02	0.14 0.11	0.07 0.05	0.05 -.02	0.16 0.0	0.03 0.02	0.07 0.05	0.02 0.0	0.0 0.0
2020	0.08 -.02	0.0 -.01	0.14 0.12	0.07 0.06	0.05 -.02	0.16 0.0	0.02 0.02	0.08 0.05	0.02 0.0	0.0 0.0
2030	0.08 -.02	0.0 0.0	0.14 0.13	0.07 0.06	0.05 -.02	0.16 0.0	0.02 0.02	0.08 0.06	0.02 0.0	0.0 0.0
2040	0.07 -.01	-.01 0.0	0.14 0.13	0.07 0.06	0.05 -.01	0.16 0.02	0.02 0.02	0.08 0.06	0.02 0.0	0.0 0.0
2050	0.06 -.03	-.02 0.0	0.14 0.14	0.07 0.07	0.05 -.01	0.15 0.03	0.02 0.02	0.08 0.07	0.02 0.0	0.0 0.0
2060	0.06 -.03	-.02 0.0	0.14 0.14	0.07 0.07	0.05 -.01	0.15 0.04	0.02 0.02	0.08 0.08	0.02 0.0	0.0 0.0
2070	0.05 -.04	-.03 0.01	0.13 0.15	0.06 0.08	0.04 -.01	0.14 0.05	0.02 0.02	0.08 0.08	0.02 0.0	0.0 0.0
2080	0.04 -.04	-.03 0.02	0.13 0.16	0.06 0.08	0.04 -.01	0.13 0.06	0.02 0.02	0.08 0.09	0.02 0.0	0.0 0.0
2090	0.03 -.04	-.04 0.02	0.13 0.16	0.06 0.08	0.04 -.01	0.12 0.06	0.01 0.02	0.07 0.09	0.02 -.01	0.0 0.0
2100	0.03 -.04	-.04 0.03	0.13 0.17	0.06 0.09	0.04 -.01	0.11 0.07	0.01 0.02	0.07 0.10	0.02 -.01	0.0 0.0
2110	0.02 -.04	-.05 0.03	0.13 0.17	0.06 0.09	0.04 0.0	0.10 0.07	0.01 0.01	0.06 0.10	0.02 -.01	0.0 0.0
2120	0.01 -.04	-.05 0.04	0.13 0.18	0.06 0.09	0.04 0.0	0.09 0.07	0.0 0.01	0.06 0.10	0.02 -.01	0.0 0.0
2130	0.0 -.04	-.05 0.04	0.13 0.18	0.06 0.10	0.04 0.0	0.08 0.07	0.0 0.01	0.05 0.10	0.02 -.01	0.0 0.0
2140	0.0 -.04	-.05 0.05	0.12 0.19	0.06 0.10	0.04 0.0	0.07 0.07	0.0 0.0	0.05 0.10	0.02 -.02	0.0 0.0
2150	-.01 -.04	-.06 0.06	0.12 0.19	0.05 0.11	0.04 0.0	0.07 0.07	0.0 0.0	0.05 0.10	0.02 -.02	0.0 0.0
2160	-.02 -.04	-.06 0.06	0.12 0.20	0.05 0.11	0.04 0.0	0.06 0.07	0.0 0.0	0.06 0.10	0.02 -.02	0.0 0.0
2170	-.03 -.04	-.06 0.07	0.12 0.20	0.05 0.11	0.04 0.0	0.05 0.06	0.0 0.0	0.06 0.10	0.02 -.02	0.0 0.0

Table 4 (continued)
(d) $\bar{K}N \to \Sigma\pi$ $I = 1$

ENERGY	S11	P11	P13	D13	D15	F15	F17	G17	G19	H19
1480	0.20 0.34	0.0 -.01	0.07 -.02	0.0 0.0	0.0 0.0	0.0 0.0	0.0 0.0	0.0 0.0	0.0 0.0	0.0 0.0
1490	0.20 0.33	0.0 -.01	0.07 -.02	0.0 0.0	0.0 0.0	0.0 0.0	0.0 0.0	0.0 0.0	0.0 0.0	0.0 0.0
1500	0.20 0.33	-.01 -.02	0.07 -.02	0.0 0.0	0.0 0.0	0.0 0.0	0.0 0.0	0.0 0.0	0.0 0.0	0.0 0.0
1510	0.21 0.32	-.02 -.02	0.07 -.02	0.0 0.0	0.0 0.0	0.0 0.0	0.0 0.0	0.0 0.0	0.0 0.0	0.0 0.0
1520	0.21 0.31	-.02 -.02	0.07 -.02	0.0 0.0	0.01 0.0	0.0 0.0	0.0 0.0	0.0 0.0	0.0 0.0	0.0 0.0
1530	0.21 0.31	-.03 -.02	0.07 -.02	0.0 0.0	0.01 0.0	0.0 0.0	0.0 0.0	0.0 0.0	0.0 0.0	0.0 0.0
1540	0.22 0.30	-.03 -.02	0.07 -.02	0.0 0.0	0.02 0.0	0.0 0.0	0.0 0.0	0.0 0.0	0.0 0.0	0.0 0.0
1550	0.22 0.29	-.04 -.02	0.07 -.03	0.0 0.0	0.02 0.0	0.0 0.0	0.0 0.0	0.0 0.0	0.0 0.0	0.0 0.0
1560	0.22 0.29	-.04 -.03	0.07 -.03	0.0 0.0	0.02 0.0	0.0 0.0	0.0 0.0	0.0 0.0	0.0 0.0	0.0 0.0
1570	0.22 0.28	-.05 -.03	0.07 -.03	0.01 0.0	0.03 0.0	0.0 0.0	0.0 0.0	0.0 0.0	0.0 0.0	0.0 0.0
1580	0.22 0.27	-.05 -.04	0.07 -.03	0.02 0.0	0.03 -.01	0.0 0.0	0.0 0.0	0.0 0.0	0.0 0.0	0.0 0.0
1590	0.22 0.27	-.06 -.04	0.07 -.03	0.02 0.01	0.03 -.01	0.0 0.0	0.0 0.0	0.0 0.0	0.0 0.0	0.0 0.0
1600	0.22 0.26	-.06 -.05	0.08 -.03	0.03 0.01	0.04 -.01	0.0 0.0	0.0 0.0	0.0 0.0	0.0 0.0	0.0 0.0
1610	0.22 0.26	-.07 -.06	0.08 -.03	0.04 0.02	0.04 -.01	0.0 0.0	0.0 0.0	0.0 0.0	0.0 0.0	0.0 0.0
1620	0.22 0.25	-.07 -.08	0.09 -.03	0.05 0.01	0.05 -.01	0.0 0.0	0.0 0.0	0.0 0.0	0.0 0.0	0.0 0.0
1630	0.22 0.24	-.07 -.09	0.08 -.03	0.07 0.04	0.05 0.0	0.0 0.0	0.0 0.0	0.0 0.0	0.0 0.0	0.0 0.0
1640	0.22 0.24	-.07 -.11	0.08 -.03	0.08 0.07	0.06 0.0	-.01 0.0	0.0 0.0	0.0 0.0	0.0 0.0	0.0 0.0
1650	0.22 0.23	-.06 -.13	0.08 -.03	0.08 0.11	0.06 0.0	-.01 0.0	-.01 0.0	0.0 0.0	0.0 0.0	0.0 0.0
1660	0.22 0.23	-.04 -.15	0.08 -.03	0.05 0.17	0.07 0.0	-.01 0.0	-.01 0.0	0.0 0.0	0.0 0.0	0.0 0.0
1670	0.22 0.22	-.01 -.16	0.08 -.03	-.02 0.20	0.07 0.0	-.02 0.0	-.01 0.0	0.0 0.0	0.0 0.0	0.0 0.0
1680	0.21 0.22	0.01 -.16	0.08 -.03	-.09 0.17	0.08 0.0	-.02 0.0	-.01 0.0	0.0 0.0	0.0 0.0	0.0 0.0
1690	0.21 0.21	0.04 -.15	0.08 -.03	-.12 0.13	0.09 0.01	-.02 -.01	-.02 0.0	0.0 0.0	0.0 0.0	0.0 0.0
1700	0.20 0.21	0.05 -.14	0.08 -.03	-.12 0.09	0.09 0.02	-.02 -.01	-.02 0.0	0.0 0.0	0.0 0.0	0.0 0.0
1710	0.20 0.20	0.07 -.12	0.08 -.03	-.12 0.06	0.10 0.03	-.02 -.01	-.02 0.0	0.0 0.0	0.0 0.0	0.0 0.0
1720	0.19 0.19	0.07 -.11	0.08 -.03	-.11 0.04	0.10 0.04	-.02 -.02	-.02 0.0	0.0 0.0	0.0 0.0	0.0 0.0
1730	0.18 0.18	0.08 -.09	0.08 -.03	-.11 0.03	0.10 0.06	-.03 -.02	-.02 0.0	0.0 0.0	0.0 0.0	0.0 0.0
1740	0.17 0.17	0.08 -.08	0.08 -.03	-.10 0.02	0.10 0.08	-.03 -.02	-.02 0.0	0.0 0.0	0.0 0.0	0.0 0.0
1750	0.16 0.15	0.08 -.07	0.08 -.03	-.10 0.01	0.08 0.09	-.03 -.02	-.02 0.0	0.0 -.01	0.0 0.0	0.0 0.0
1760	0.16 0.12	0.08 -.06	0.08 -.03	-.09 0.0	0.07 0.10	-.03 -.02	-.02 0.01	0.0 -.01	0.0 0.0	0.0 0.0
1770	0.18 0.10	0.07 -.06	0.08 -.03	-.09 0.0	0.05 0.11	-.04 -.03	-.02 0.01	0.0 -.01	0.0 0.0	0.0 0.0
1780	0.20 0.09	0.07 -.05	0.08 -.03	-.08 0.0	0.03 0.11	-.04 -.03	-.02 0.01	0.0 -.02	0.0 0.0	0.0 0.0
1790	0.22 0.10	0.07 -.04	0.09 -.03	-.08 -.01	0.02 0.10	-.04 -.03	-.02 0.01	0.0 -.02	0.0 0.0	0.0 0.0
1800	0.22 0.11	0.07 -.04	0.09 -.03	-.07 -.02	0.0 0.09	-.05 -.04	-.02 0.01	0.0 -.02	0.0 0.0	0.0 0.0
1810	0.22 0.12	0.06 -.03	0.09 -.03	-.06 -.02	0.0 0.08	-.05 -.04	-.03 0.01	0.0 -.02	0.0 0.0	0.0 0.0
1820	0.22 0.13	0.06 -.03	0.09 -.03	-.06 -.03	-.01 0.07	-.06 -.05	-.03 0.01	0.0 -.02	0.0 0.0	0.0 0.0
1830	0.21 0.13	0.06 -.01	0.09 -.03	-.05 -.03	-.01 0.06	-.06 -.06	-.03 0.01	0.0 -.03	0.0 0.0	0.0 0.0
1840	0.20 0.14	0.06 -.02	0.09 -.03	-.05 -.01	-.01 0.05	-.06 -.07	-.03 0.01	0.0 -.03	0.0 0.0	0.0 0.0
1850	0.19 0.14	0.05 -.02	0.09 -.03	-.04 -.03	-.01 0.04	-.07 -.08	-.03 0.0	0.01 -.03	0.0 0.0	0.0 0.0
1860	0.18 0.15	0.05 -.02	0.09 -.03	-.03 -.03	-.01 0.03	-.07 -.10	-.03 0.0	0.01 -.03	0.0 0.0	0.0 0.0
1870	0.16 0.15	0.05 -.02	0.09 -.03	-.03 -.03	-.01 0.03	-.07 -.12	-.03 0.0	0.02 -.03	0.0 0.0	0.0 0.0
1880	0.14 0.15	0.05 -.01	0.09 -.03	-.02 -.03	0.0 0.02	-.06 -.14	-.04 0.0	0.02 -.03	0.0 0.0	0.0 0.0
1890	0.13 0.16	0.05 -.01	0.09 -.03	-.02 -.03	0.0 0.02	-.05 -.16	-.04 0.0	0.02 -.03	0.0 0.0	0.0 0.0
1900	0.10 0.15	0.04 -.01	0.09 -.03	-.01 -.03	0.0 0.01	-.01 -.18	-.04 0.0	0.03 -.03	0.0 0.0	0.0 0.0
1910	0.08 0.15	0.04 0.0	0.09 -.03	0.0 -.03	0.0 0.01	0.0 -.19	-.04 0.0	0.03 -.03	0.0 0.0	0.0 0.0
1920	0.06 0.14	0.04 0.0	0.09 -.03	0.0 -.02	0.0 0.0	0.03 -.20	-.05 -.01	0.04 -.03	0.0 0.0	0.0 0.0
1930	0.03 0.13	0.04 0.0	0.09 -.03	0.0 -.02	0.0 0.0	0.06 -.19	-.05 -.02	0.04 -.02	0.0 0.0	0.0 0.0
1940	0.01 0.11	0.04 0.0	0.09 -.03	0.0 -.01	0.0 0.0	0.09 -.18	-.05 -.03	0.04 -.02	0.0 0.0	0.0 0.0
1950	0.0 0.09	0.04 0.0	0.09 -.03	0.0 -.01	0.0 0.0	0.11 -.16	-.05 -.04	0.05 -.02	0.0 0.0	0.0 0.0
1960	-.02 0.07	0.03 0.0	0.09 -.03	0.01 0.0	0.01 0.0	0.12 -.14	-.05 -.05	0.05 -.02	0.0 0.0	0.0 0.0
1970	-.03 0.04	0.03 0.0	0.09 -.03	0.01 0.0	0.01 0.0	0.13 -.13	-.05 -.06	0.05 -.02	0.0 0.0	0.0 0.0
1980	-.04 0.02	0.03 0.0	0.09 -.03	0.01 0.0	0.02 0.0	0.13 -.11	-.05 -.07	0.06 -.01	0.0 0.0	0.0 0.0
1990	-.04 0.0	0.03 0.0	0.10 -.03	0.01 0.0	0.02 0.0	0.14 -.10	-.05 -.08	0.06 0.0	0.0 0.0	0.0 0.0
2000	-.03 -.02	0.03 0.0	0.10 -.03	0.01 0.0	0.02 0.0	0.14 -.08	-.04 -.09	0.06 0.0	0.0 0.0	0.0 0.0
2010	-.03 -.04	0.03 0.0	0.10 -.03	0.01 0.01	0.02 0.0	0.14 -.07	-.03 -.10	0.06 0.0	0.0 0.0	0.0 0.0
2020	-.02 -.05	0.03 0.0	0.10 -.03	0.01 0.02	0.02 -.01	0.13 -.06	-.02 -.11	0.07 0.0	0.0 0.0	0.0 0.0
2030	-.02 -.06	0.02 0.0	0.10 -.04	0.01 0.02	0.03 -.01	0.13 -.05	0.0 -.11	0.07 0.0	0.0 0.0	0.0 0.0
2040	-.01 -.07	0.02 0.0	0.10 -.04	0.01 0.02	0.03 -.01	0.13 -.04	0.01 -.11	0.07 0.0	0.0 0.0	0.0 0.0
2050	0.0 -.07	0.02 0.0	0.10 -.04	0.0 0.02	0.03 -.01	0.13 -.03	0.02 -.11	0.07 0.01	0.0 0.0	0.0 0.0
2060	0.0 -.08	0.02 0.0	0.10 -.04	0.0 0.03	0.03 -.01	0.12 -.02	0.04 -.10	0.07 0.01	0.0 0.0	0.0 0.0
2070	0.0 -.08	0.02 0.0	0.10 -.04	0.0 0.03	0.03 -.02	0.12 -.02	0.04 -.10	0.07 0.02	0.0 0.0	0.0 0.0
2080	0.0 -.08	0.02 0.01	0.10 -.04	0.0 0.03	0.03 -.02	0.12 0.0	0.05 -.09	0.07 0.02	0.0 0.0	0.0 0.0
2090	0.0 -.08	0.02 0.01	0.10 -.04	0.0 0.03	0.04 -.02	0.11 0.0	0.05 -.08	0.07 0.02	0.0 0.0	0.0 0.0
2100	0.0 -.09	0.02 0.01	0.10 -.04	0.0 0.03	0.04 -.02	0.11 0.0	0.06 -.07	0.07 0.03	0.0 0.0	0.0 0.0
2110	0.0 -.09	0.02 0.01	0.10 -.04	0.0 0.04	0.04 -.02	0.10 0.0	0.06 -.06	0.07 0.03	0.0 0.0	0.0 0.0
2120	0.0 -.08	0.02 0.01	0.10 -.04	0.0 0.04	0.04 -.02	0.10 0.01	0.05 -.06	0.07 0.03	0.0 0.0	0.0 0.0
2130	0.0 -.08	0.01 0.01	0.10 -.04	0.0 0.04	0.04 -.02	0.09 0.02	0.05 -.05	0.07 0.03	0.0 0.0	0.0 0.0
2140	0.0 -.08	0.01 0.02	0.10 -.04	0.0 0.04	0.04 -.02	0.09 0.02	0.05 -.05	0.07 0.04	0.0 0.0	0.0 0.0
2150	0.0 -.08	0.01 0.02	0.10 -.04	0.0 0.04	0.04 -.02	0.08 0.02	0.04 -.05	0.07 0.04	0.0 0.0	0.0 0.0
2160	0.0 -.08	0.01 0.02	0.10 -.04	0.0 0.04	0.05 -.02	0.08 0.03	0.04 -.05	0.07 0.04	0.0 0.0	0.0 0.0
2170	0.0 -.08	0.01 0.02	0.10 -.04	0.0 0.04	0.05 -.02	0.07 0.03	0.03 -.05	0.07 0.04	0.0 0.0	0.0 0.0

Table 4 (continued)
(e) $\bar{K}N \to \Lambda\pi$

ENERGY	S11	P11	P13	D13	D15	F15	F17	G17	G19	H19
1480	-.24 -.16	-.05 -.02	-.06 -.02	-.01 0.0	0.0 0.0	0.0 0.0	0.0 0.0	0.0 0.0	0.0 0.0	0.0 0.0
1490	-.24 -.15	-.06 -.03	-.06 -.01	0.0 0.0	0.0 0.0	0.0 0.0	0.0 0.0	0.0 0.0	0.0 0.0	0.0 0.0
1500	-.24 -.15	-.07 -.03	-.06 0.0	0.0 0.0	-.01 0.0	0.0 0.0	0.0 0.0	0.0 0.0	0.0 0.0	0.0 0.0
1510	-.24 -.14	-.08 -.04	-.06 0.0	0.0 0.0	-.01 0.0	0.0 0.0	0.0 0.0	0.0 0.0	0.0 0.0	0.0 0.0
1520	-.24 -.14	-.09 -.04	-.06 0.0	0.0 0.0	-.02 0.0	0.0 0.0	0.0 0.0	0.0 0.0	0.0 0.0	0.0 0.0
1530	-.24 -.13	-.10 -.05	-.07 0.01	0.0 0.0	-.02 0.0	0.0 0.0	0.0 0.0	0.0 0.0	0.0 0.0	0.0 0.0
1540	-.24 -.13	-.10 -.05	-.07 0.02	0.0 0.0	-.02 0.0	0.0 0.0	0.0 0.0	0.0 0.0	0.0 0.0	0.0 0.0
1550	-.24 -.12	-.11 -.06	-.07 0.02	0.0 0.0	-.03 0.0	0.0 0.0	0.0 0.0	0.0 0.0	0.0 0.0	0.0 0.0
1560	-.24 -.12	-.12 -.06	-.06 0.03	0.0 0.01	-.03 0.0	0.0 0.0	0.0 0.0	0.0 0.0	0.0 0.0	0.0 0.0
1570	-.24 -.11	-.12 -.07	-.06 0.04	0.0 0.02	-.04 0.0	0.0 0.0	0.0 0.0	0.0 0.0	0.0 0.0	0.0 0.0
1580	-.24 -.11	-.13 -.07	-.06 0.04	0.0 0.02	-.04 0.0	0.0 0.0	0.0 0.0	0.0 0.0	0.0 0.0	0.0 0.0
1590	-.24 -.10	-.14 -.08	-.06 0.05	0.0 0.02	-.05 -.01	0.0 0.0	0.0 0.0	0.0 0.0	0.0 0.0	0.0 0.0
1600	-.24 -.10	-.14 -.09	-.05 0.05	0.0 0.03	-.05 -.01	0.0 0.0	0.01 0.0	0.0 0.0	0.0 0.0	0.0 0.0
1610	-.24 -.09	-.15 -.09	-.05 0.06	0.0 0.04	-.06 -.02	0.0 0.0	0.01 0.0	0.0 0.0	0.0 0.0	0.0 0.0
1620	-.24 -.09	-.15 -.09	-.05 0.06	0.0 0.05	-.07 -.02	0.0 0.0	0.01 0.0	0.0 0.0	0.0 0.0	0.0 0.0
1630	-.24 -.08	-.16 -.09	-.04 0.07	0.0 0.06	-.08 -.02	0.0 0.0	0.02 0.0	0.0 0.0	0.0 0.0	0.0 0.0
1640	-.24 -.08	-.16 -.10	-.04 0.07	0.0 0.07	-.08 -.03	0.0 0.0	0.02 0.0	0.0 0.0	0.0 0.0	0.0 0.0
1650	-.23 -.08	-.17 -.10	-.03 0.08	-.03 0.09	-.09 -.03	0.0 0.0	0.02 0.0	0.0 0.0	0.0 0.0	0.0 0.0
1660	-.23 -.07	-.17 -.11	-.03 0.08	-.06 0.10	-.10 -.04	0.0 0.0	0.02 0.0	0.0 0.0	0.0 0.0	0.0 0.0
1670	-.23 -.07	-.18 -.11	-.02 0.08	-.09 0.08	-.11 -.05	-.01 0.0	0.02 0.0	0.0 0.0	0.0 0.0	0.0 0.0
1680	-.23 -.06	-.18 -.11	-.02 0.08	-.10 0.05	-.12 -.06	-.01 0.0	0.03 0.0	0.0 0.0	0.0 0.0	0.0 0.0
1690	-.22 -.06	-.19 -.11	0.0 0.09	-.09 0.02	-.14 -.08	-.01 0.0	0.03 0.0	0.0 0.0	0.0 0.0	0.0 0.0
1700	-.22 -.06	-.19 -.12	0.0 0.09	-.08 0.01	-.14 -.10	-.01 0.0	0.03 0.0	0.0 0.0	0.0 0.0	0.0 0.0
1710	-.22 -.05	-.19 -.12	0.0 0.09	-.07 0.0	-.15 -.12	-.02 0.0	0.03 0.0	0.0 0.0	0.0 0.0	0.0 0.0
1720	-.21 -.05	-.20 -.12	0.0 0.09	-.07 0.0	-.15 -.15	-.02 0.0	0.04 0.0	0.0 0.0	0.0 0.0	0.0 0.0
1730	-.21 -.05	-.20 -.12	0.01 0.09	-.06 0.0	-.15 -.18	-.02 0.0	0.04 0.0	0.0 0.0	0.0 0.0	0.0 0.0
1740	-.20 -.04	-.20 -.12	0.02 0.09	-.06 0.0	-.14 -.22	-.02 0.0	0.04 0.0	0.0 0.0	0.0 0.0	0.0 0.0
1750	-.19 -.03	-.21 -.12	0.02 0.09	-.06 0.0	-.11 -.25	-.02 0.0	0.04 0.0	0.0 0.0	0.0 0.0	0.0 0.0
1760	-.19 -.02	-.21 -.12	0.04 0.08	-.06 0.0	-.07 -.27	-.02 0.0	0.05 0.0	0.0 0.0	0.0 0.0	0.0 0.0
1770	-.19 0.0	-.21 -.13	0.03 0.08	-.06 0.0	-.03 -.28	-.03 0.0	0.05 0.0	0.0 0.0	0.0 0.0	0.0 0.0
1780	-.19 0.0	-.21 -.13	0.04 0.08	-.06 0.0	0.0 -.28	-.03 0.0	0.05 0.0	0.0 0.0	0.0 0.0	0.0 0.0
1790	-.20 0.0	-.22 -.13	0.04 0.08	-.06 0.0	0.04 -.27	-.03 0.0	0.06 0.0	0.0 0.0	0.0 0.0	0.0 0.0
1800	-.20 0.0	-.22 -.12	0.05 0.08	-.07 0.0	0.07 -.25	-.03 -.01	0.06 0.0	0.0 0.0	0.0 0.0	0.0 0.0
1810	-.20 0.0	-.22 -.12	0.05 0.07	-.07 0.0	0.09 -.23	-.03 -.02	0.06 0.0	0.0 0.0	0.0 0.0	0.0 0.0
1820	-.20 0.0	-.22 -.12	0.05 0.07	-.07 0.0	0.10 -.20	-.04 -.02	0.07 0.0	0.0 0.0	0.0 0.0	0.0 0.0
1830	-.19 0.0	-.22 -.12	0.06 0.07	-.07 0.0	0.11 -.18	-.04 -.02	0.07 0.0	0.0 0.0	0.0 0.0	0.0 0.0
1840	-.19 0.0	-.22 -.12	0.06 0.07	-.07 0.0	0.11 -.16	-.04 -.03	0.08 0.0	0.0 0.0	0.0 0.0	0.0 0.0
1850	-.18 0.0	-.22 -.12	0.06 0.06	-.07 0.0	0.11 -.14	-.03 -.04	0.08 0.0	-.01 0.0	0.0 0.0	0.0 0.0
1860	-.18 0.0	-.23 -.12	0.06 0.06	-.07 0.0	0.11 -.13	-.03 -.04	0.08 0.0	-.01 0.0	0.0 0.0	0.0 0.0
1870	-.17 0.01	-.23 -.11	0.07 0.06	-.07 0.0	0.11 -.12	-.02 -.05	0.09 0.0	-.01 0.0	0.0 0.0	0.0 0.0
1880	-.16 0.01	-.23 -.11	0.07 0.05	-.07 0.0	0.11 -.11	-.02 -.05	0.09 0.01	-.01 0.0	0.0 0.0	0.0 0.0
1890	-.15 0.02	-.23 -.11	0.07 0.05	-.07 0.0	0.10 -.10	0.0 -.06	0.10 0.01	-.01 0.0	0.0 0.0	0.0 0.0
1900	-.14 0.02	-.23 -.11	0.07 0.05	-.07 -.01	0.10 -.09	0.0 -.06	0.10 0.02	-.02 0.0	0.0 0.0	0.0 0.0
1910	-.13 0.03	-.23 -.10	0.07 0.05	-.07 -.01	0.10 -.08	0.02 -.05	0.11 0.02	-.02 0.0	0.0 0.0	0.0 0.0
1920	-.13 0.03	-.23 -.10	0.07 0.04	-.07 -.01	0.09 -.07	0.03 -.04	0.11 0.03	-.02 0.0	0.0 0.0	0.0 0.0
1930	-.12 0.04	-.22 -.09	0.07 0.04	-.07 -.01	0.09 -.07	0.03 -.03	0.11 0.04	-.02 0.0	0.0 0.0	0.0 0.0
1940	-.11 0.05	-.22 -.09	0.07 0.04	-.07 -.01	0.08 -.06	0.03 -.02	0.12 0.05	-.02 0.0	0.0 0.0	0.0 0.0
1950	-.10 0.06	-.22 -.09	0.07 0.04	-.07 -.01	0.08 -.06	0.03 0.0	0.12 0.06	-.02 0.0	0.0 0.0	0.0 0.0
1960	-.10 0.07	-.22 -.08	0.07 0.03	-.07 -.01	0.08 -.05	0.03 0.0	0.12 0.07	-.02 0.0	0.0 0.0	0.0 0.0
1970	-.10 0.08	-.22 -.08	0.07 0.03	-.07 -.01	0.08 -.05	0.02 0.0	0.12 0.09	-.02 0.0	0.0 0.0	0.0 0.0
1980	-.10 0.09	-.22 -.07	0.07 0.03	-.07 -.01	0.07 -.04	0.02 0.01	0.11 0.10	-.02 0.0	0.0 0.0	0.0 0.0
1990	-.10 0.10	-.21 -.07	0.07 0.03	-.07 -.01	0.07 -.04	0.01 0.02	0.11 0.12	-.02 0.0	0.0 0.0	0.0 0.0
2000	-.10 0.11	-.21 -.06	0.07 0.03	-.07 -.01	0.07 -.03	0.0 0.02	0.10 0.13	-.02 0.0	0.0 0.0	0.0 0.0
2010	-.10 0.11	-.21 -.06	0.07 0.02	-.07 -.01	0.06 -.03	0.0 0.02	0.08 0.14	-.02 0.0	-.01 0.01	0.0 0.0
2020	-.10 0.12	-.20 -.05	0.07 0.02	-.07 -.01	0.06 -.03	0.0 0.02	0.06 0.15	-.02 0.0	-.01 0.01	0.0 0.0
2030	-.11 0.12	-.20 -.05	0.07 0.02	-.07 -.01	0.06 -.03	-.01 0.02	0.04 0.16	-.02 0.0	-.02 0.01	0.0 0.0
2040	-.11 0.12	-.19 -.04	0.07 0.02	-.07 -.01	0.06 -.02	-.02 0.02	0.02 0.16	-.02 -.01	-.02 0.02	0.0 0.0
2050	-.11 0.13	-.19 -.04	0.07 0.02	-.08 -.01	0.06 -.02	-.02 0.02	0.0 0.16	-.02 -.01	-.02 0.02	0.0 0.0
2060	-.11 0.13	-.18 -.03	0.07 0.02	-.08 -.01	0.05 -.02	-.02 0.02	-.01 0.15	-.02 -.01	-.02 0.C2	0.0 0.0
2070	-.11 0.13	-.18 -.03	0.06 0.02	-.08 -.01	0.05 -.01	-.03 0.02	-.03 0.14	-.02 -.01	-.03 0.02	0.0 0.0
2080	-.11 0.13	-.17 -.02	0.06 0.02	-.08 -.01	0.05 -.01	-.03 0.02	-.04 0.13	-.01 -.01	-.03 0.02	0.0 0.0
2090	-.11 0.13	-.16 -.02	0.06 0.01	-.09 -.02	0.05 0.0	-.03 0.02	-.05 0.12	-.01 -.01	-.03 0.02	0.0 0.0
2100	-.10 0.13	-.16 -.02	0.06 0.01	-.09 -.02	0.05 0.0	-.04 0.02	-.06 0.11	-.01 -.02	-.04 0.02	0.0 0.0
2110	-.10 0.13	-.15 -.01	0.06 0.01	-.09 -.02	0.05 0.0	-.04 0.02	-.06 0.10	-.01 -.02	-.04 0.C3	0.0 0.0
2120	-.10 0.13	-.14 0.0	0.06 0.01	-.09 -.02	0.04 0.0	-.04 0.01	-.07 0.09	0.0 -.02	-.05 0.C3	0.0 0.0
2130	-.10 0.13	-.13 0.0	0.05 0.01	-.09 -.02	0.04 0.0	-.05 0.01	-.07 0.08	0.0 -.02	-.05 0.03	0.0 0.0
2140	-.10 0.13	-.13 0.0	0.05 0.01	-.10 -.03	0.04 0.0	-.05 0.01	-.07 0.08	0.0 -.02	-.06 0.03	0.0 0.0
2150	-.09 0.13	-.12 0.0	0.05 0.01	-.10 -.03	0.04 0.0	-.05 0.0	-.08 0.07	0.0 -.02	-.06 0.03	0.0 0.0
2160	-.09 0.13	-.11 0.0	0.05 0.01	-.10 -.03	0.04 0.0	-.06 0.0	-.08 0.06	0.0 -.02	-.07 0.03	0.0 0.0
2170	-.09 0.13	-.10 0.0	0.04 0.01	-.10 -.04	0.04 0.0	-.06 0.0	-.08 0.06	0.0 -.02	-.07 0.C3	0.0 0.0

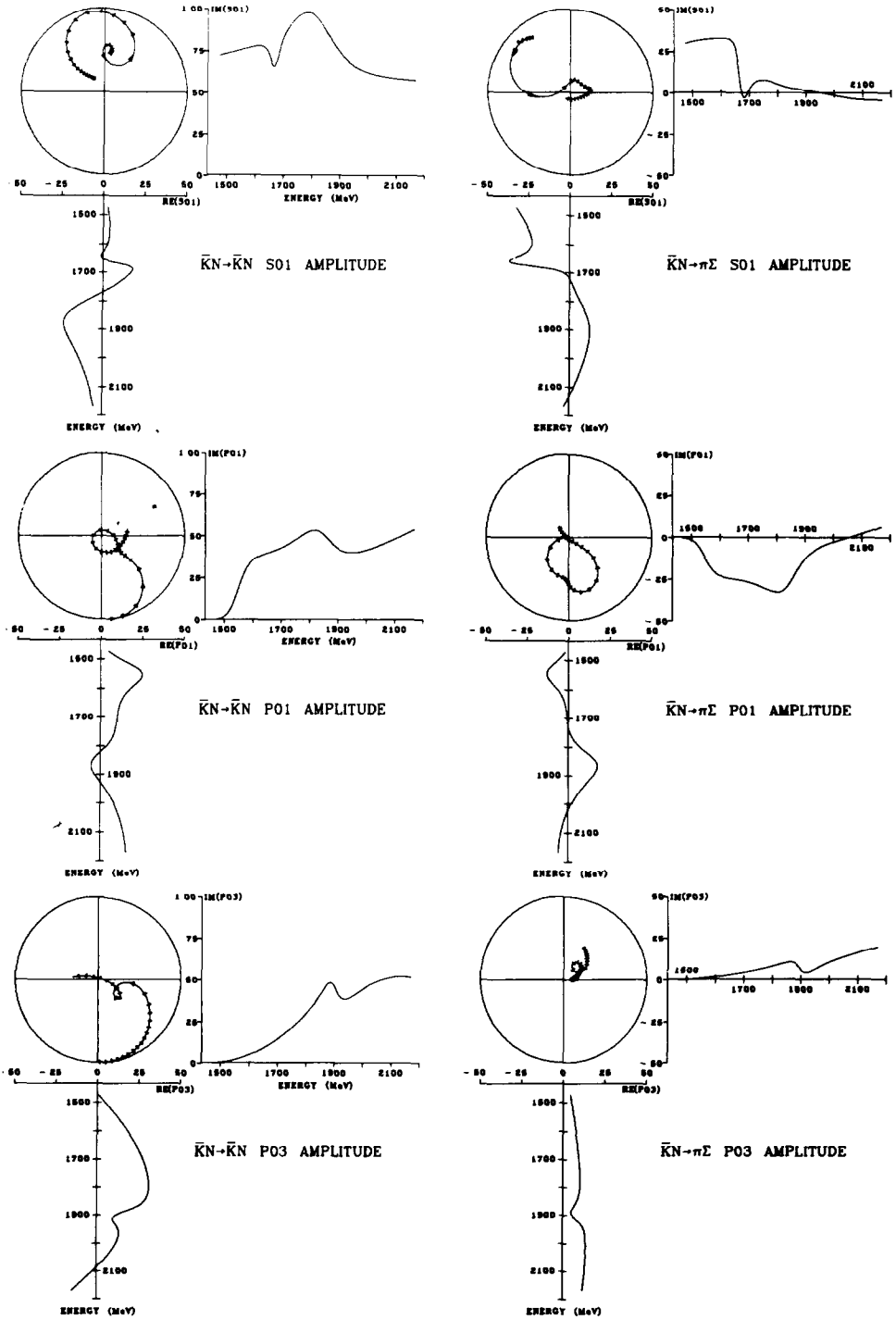
$\bar{K}N \to \bar{K}N$ S01 AMPLITUDE
$\bar{K}N \to \pi\Sigma$ S01 AMPLITUDE
$\bar{K}N \to \bar{K}N$ P01 AMPLITUDE
$\bar{K}N \to \pi\Sigma$ P01 AMPLITUDE
$\bar{K}N \to \bar{K}N$ P03 AMPLITUDE
$\bar{K}N \to \pi\Sigma$ P03 AMPLITUDE
ENERGY (MeV)

Fig. 1.

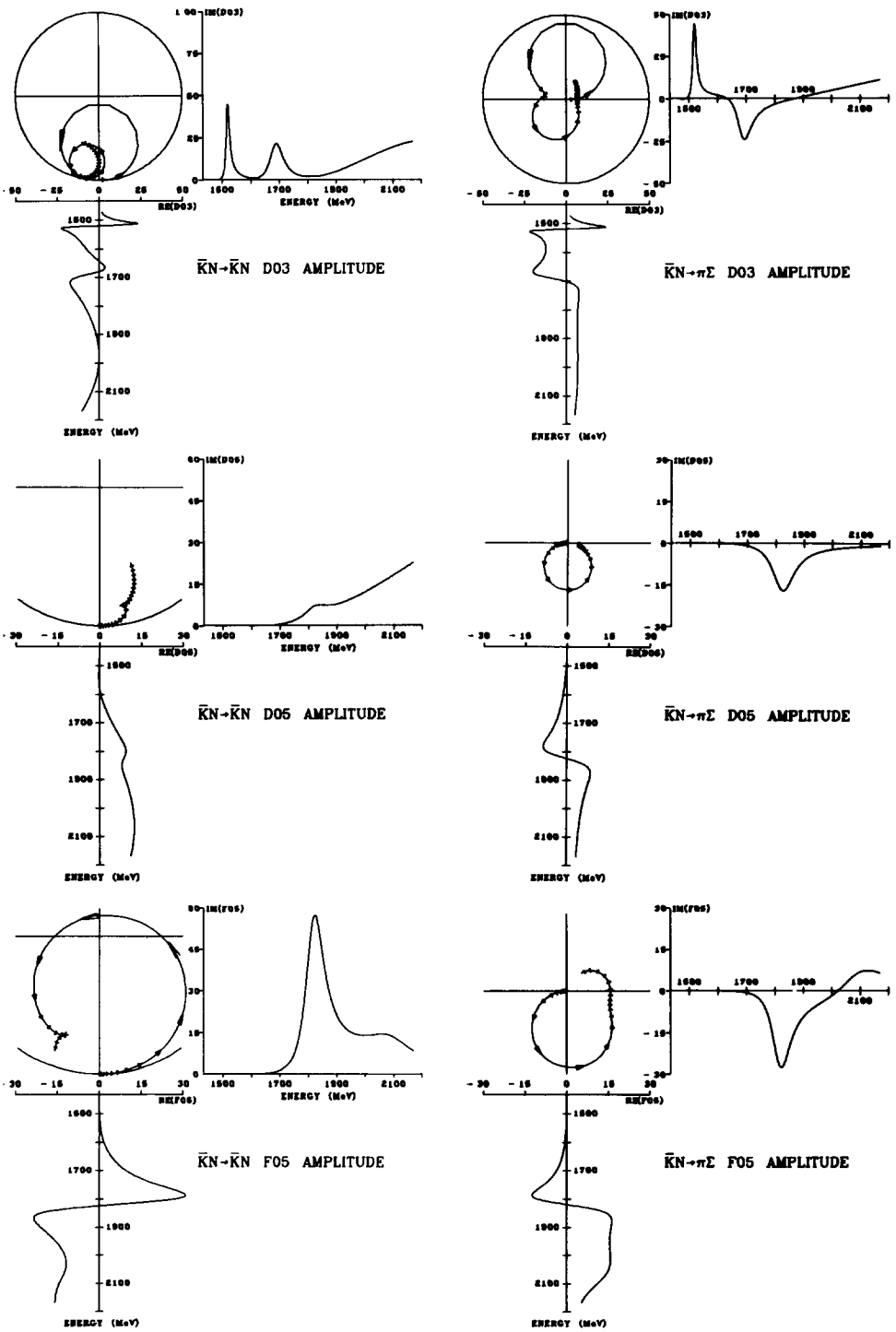

Fig. 1 (continued).

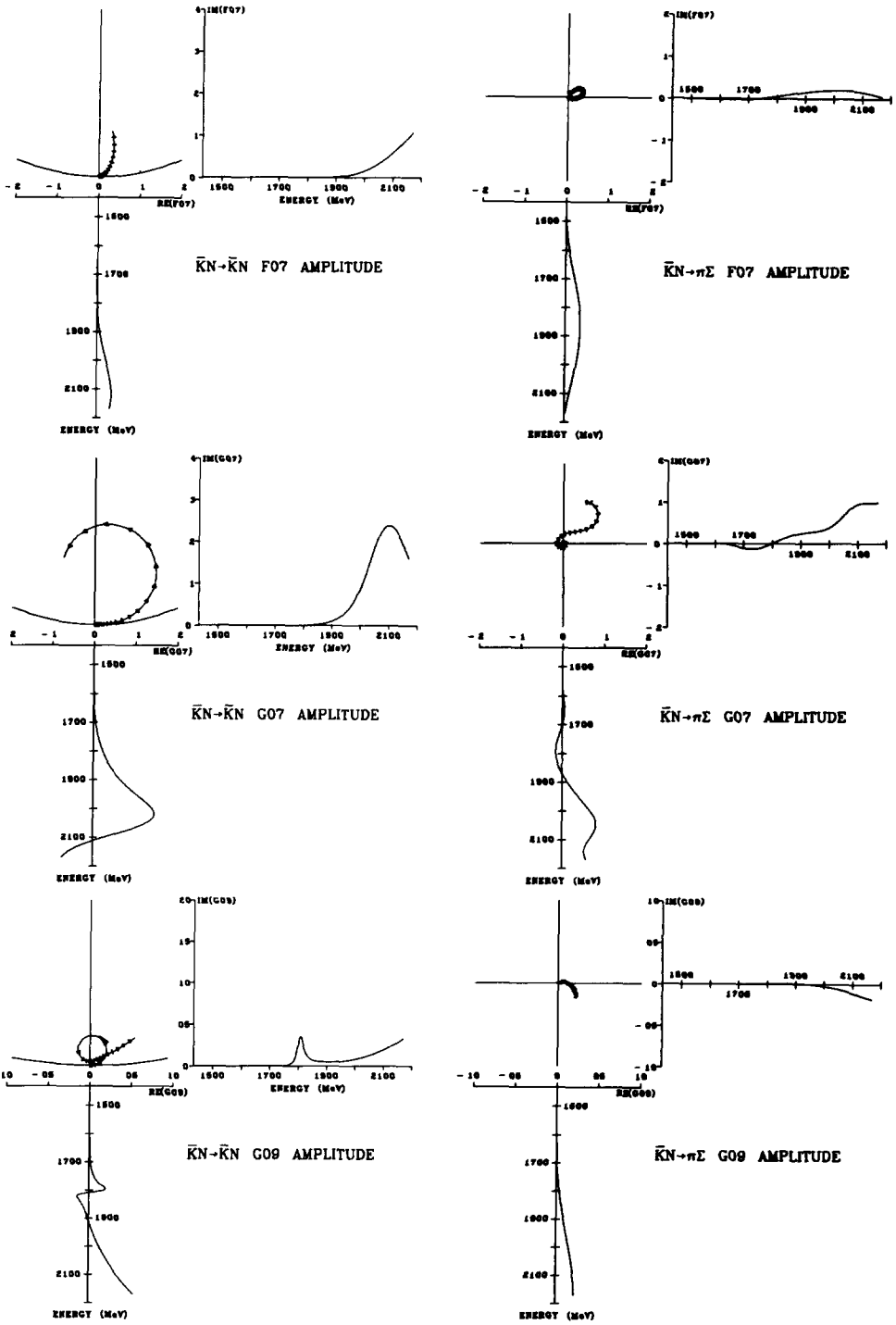

Fig. 1 (continued).

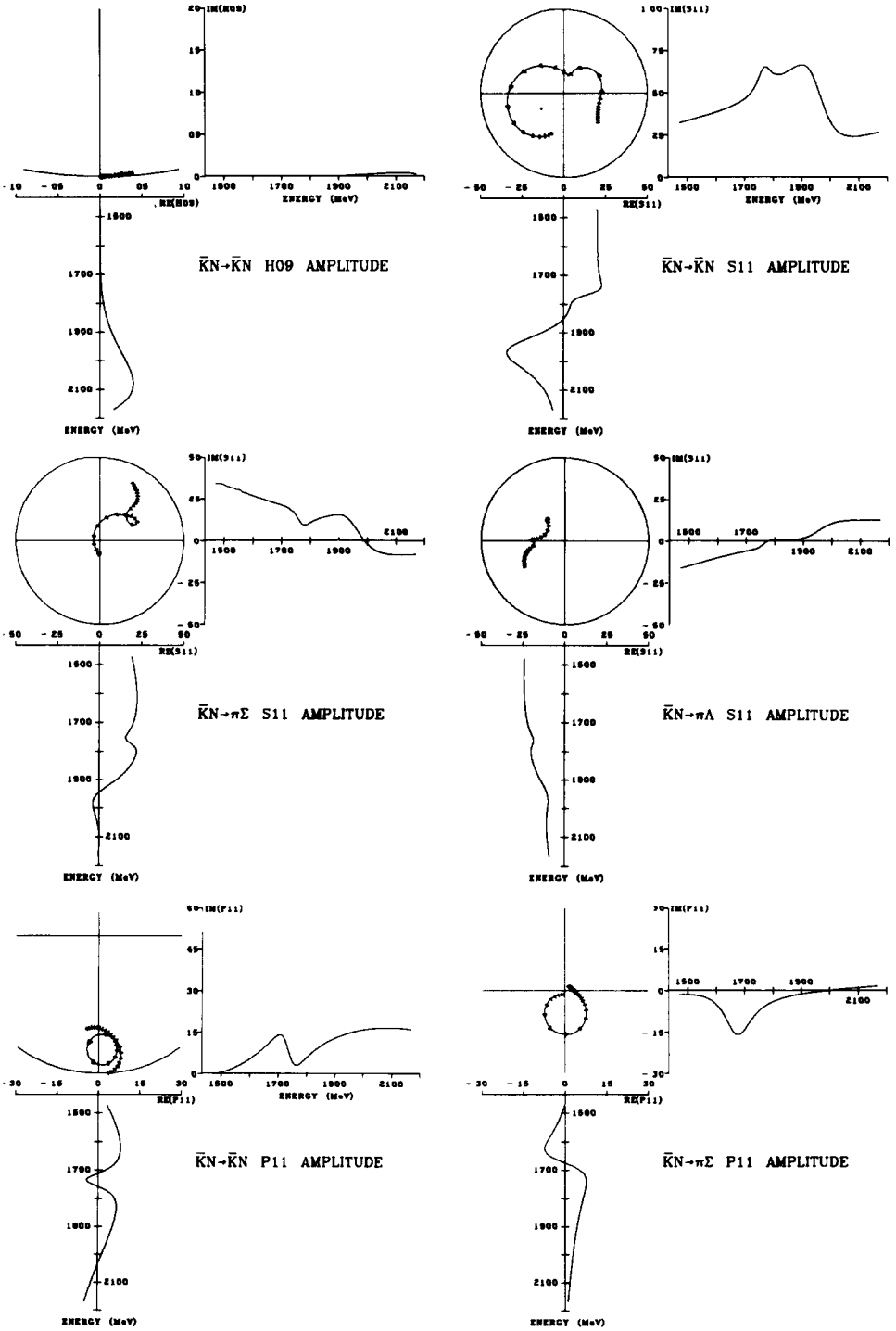

Fig. 1 (continued).

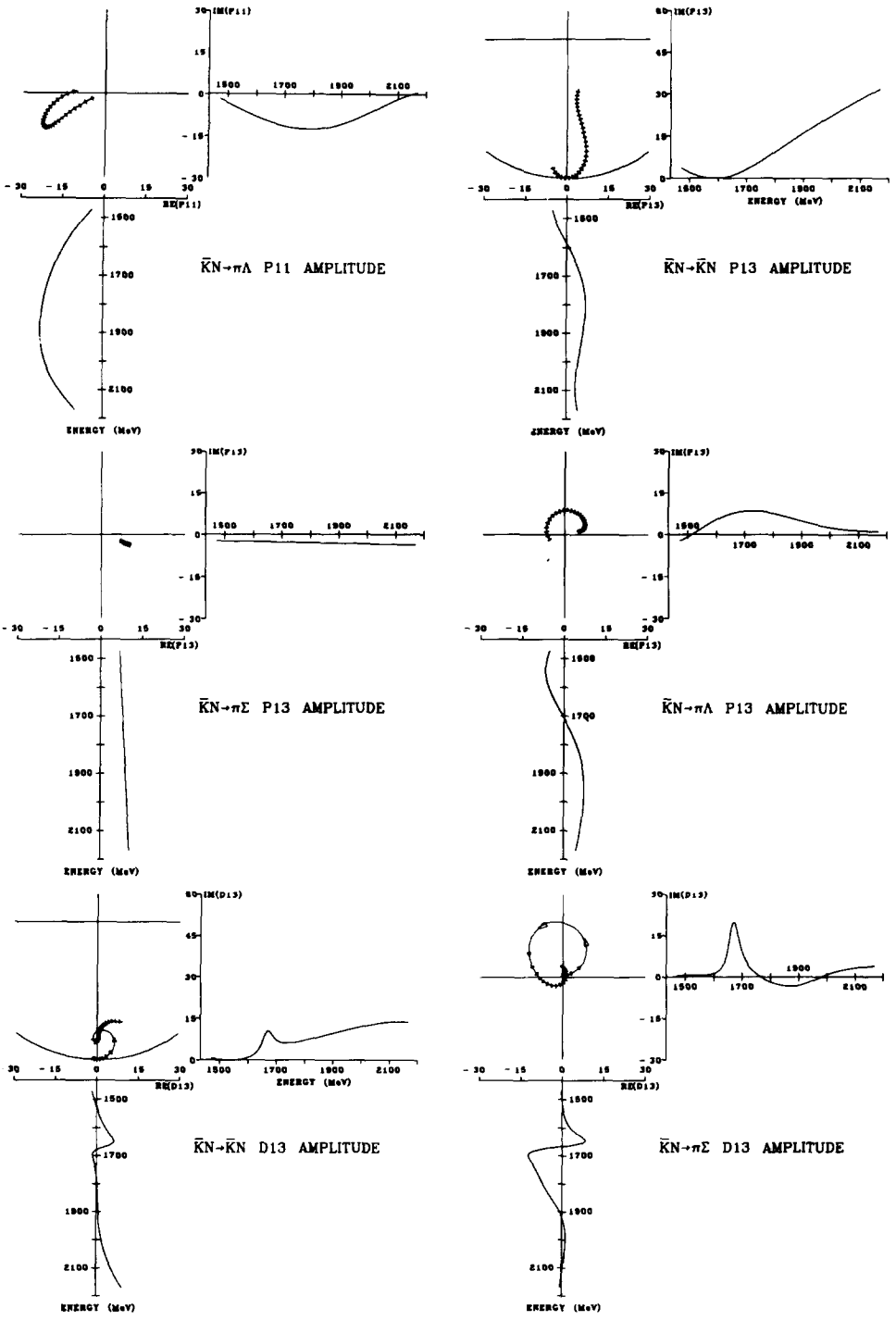

Fig. 1 (continued).

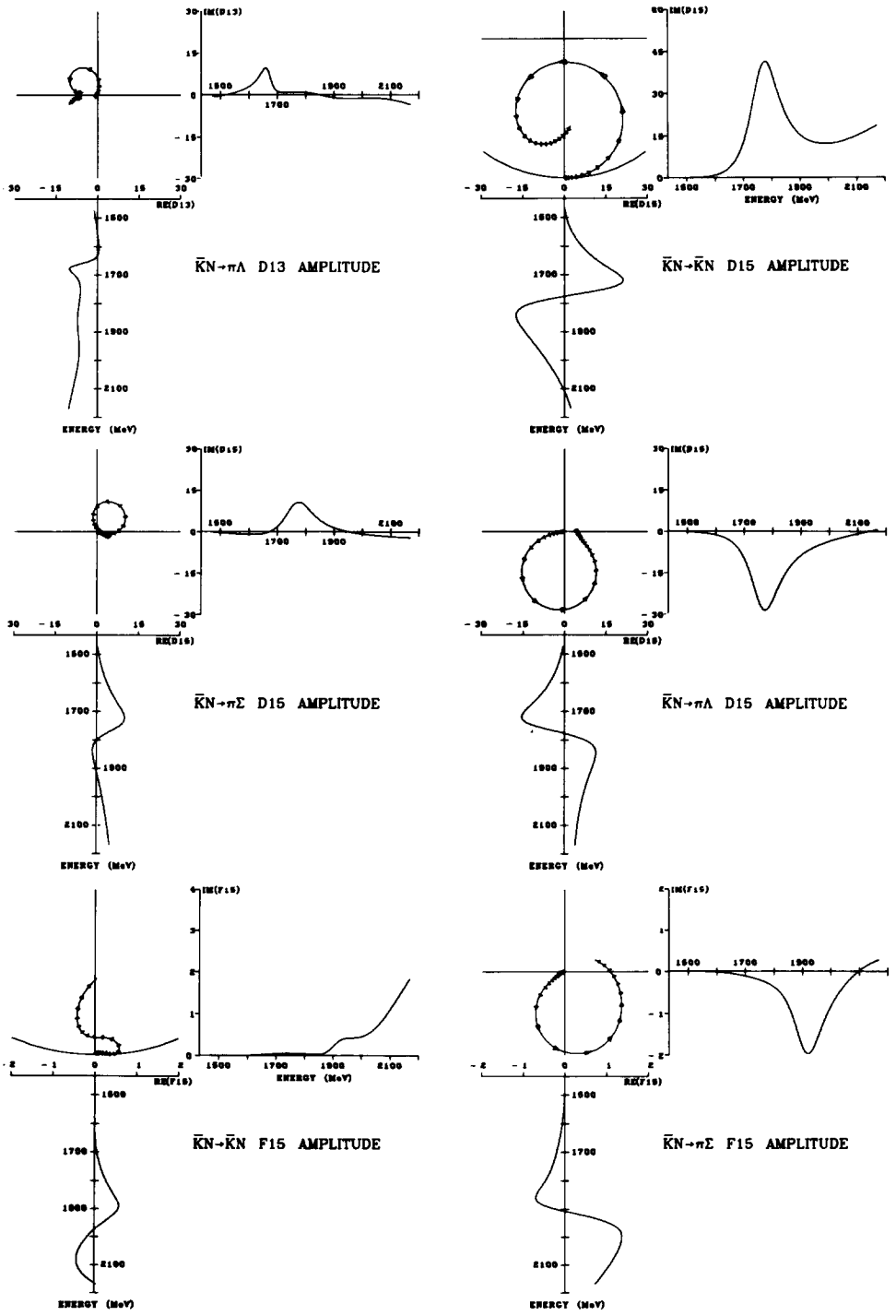

Fig. 1 (continued).

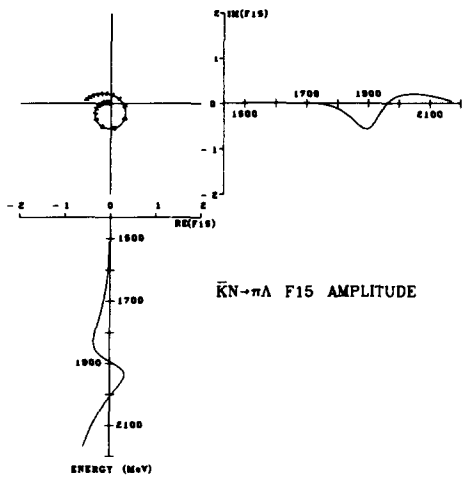

$\bar{K}N \to \pi\Lambda$ F15 AMPLITUDE

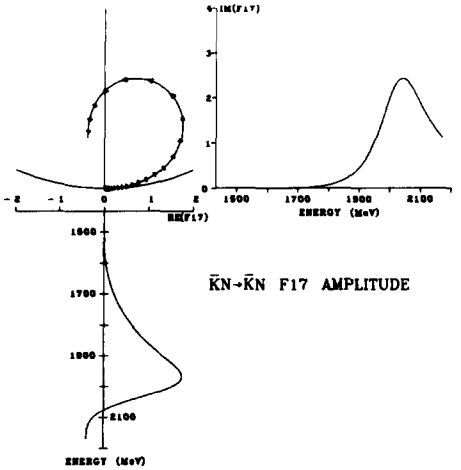

$\bar{K}N \to \bar{K}N$ F17 AMPLITUDE

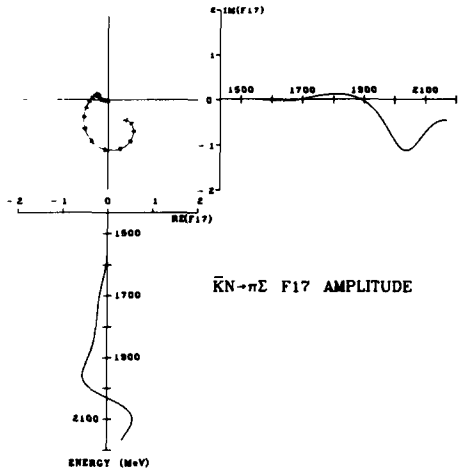

$\bar{K}N \to \pi\Sigma$ F17 AMPLITUDE

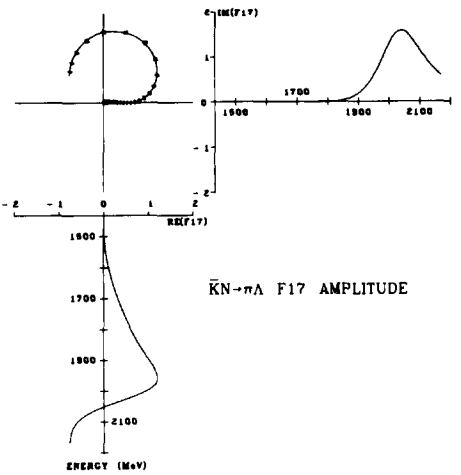

$\bar{K}N \to \pi\Lambda$ F17 AMPLITUDE

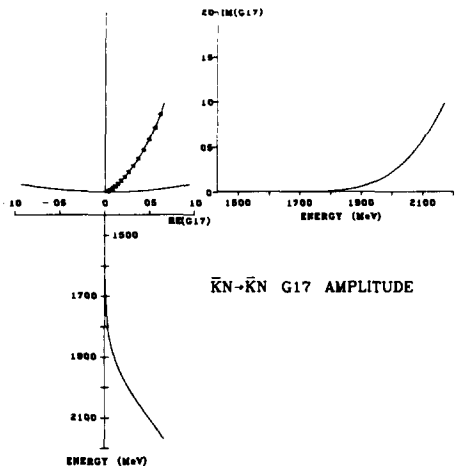

$\bar{K}N \to \bar{K}N$ G17 AMPLITUDE

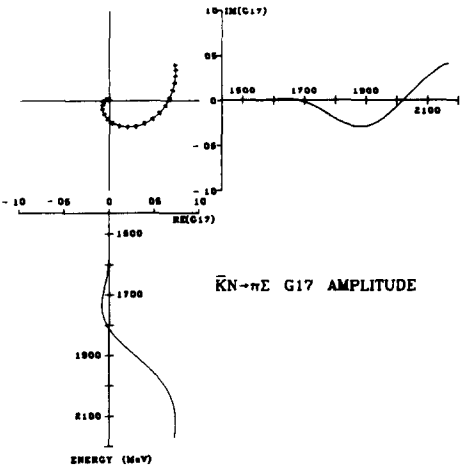

$\bar{K}N \to \pi\Sigma$ G17 AMPLITUDE

Fig. 1 (continued).

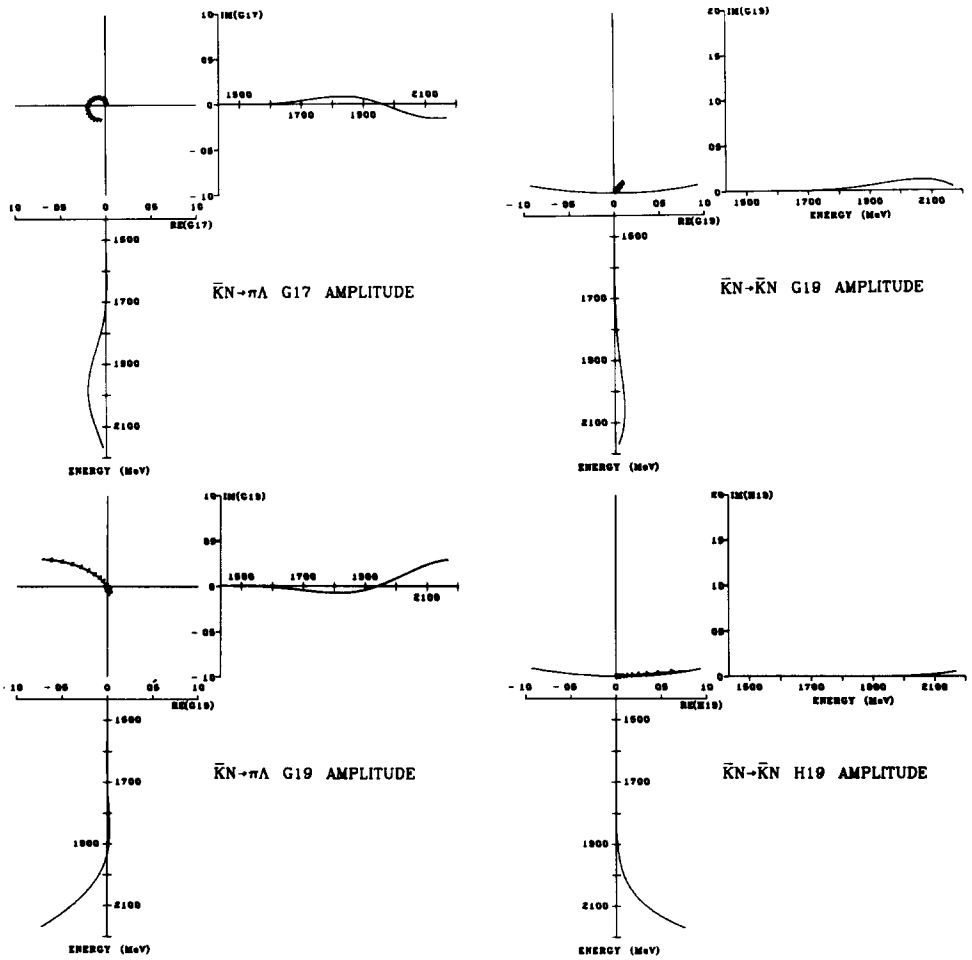

Fig. 1 (continued).

Fig. 1. The Argand diagrams for the partial wave amplitudes of the final consistent resonances solutions for $\bar{K}N \to \bar{K}N$ and $\bar{K}N \to \Sigma\pi$ for S01 to H09 and $\bar{K}N \to \bar{K}N$, $\bar{K}N \to \Sigma\pi$ and $\bar{K}N \to \Lambda\pi$ for S11 to H19. The energy dependence of each amplitude is displayed by plotting its real and imaginary parts *versus* energy in alignment with the corresponding Argand plot. In addition, arrows with bases positioned at integral multiples of 25 MeV and a base-to-tip length of 5 MeV are plotted on all the Argand plots. The energy axes run from the elastic threshold to 2200 MeV.

estimated from the spread of values between the channels and the general stability of the parameters over the full sequence of the fitting.

In most cases the resonances introduced into a solution from another channel had low couplings, usually <0.03 (about the level of sensitivity of the solutions for

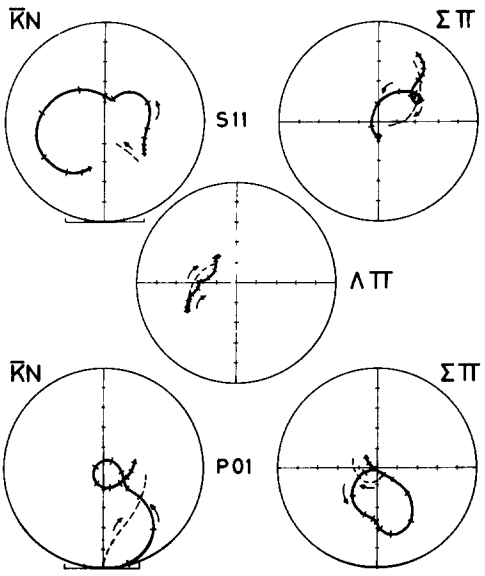

Fig. 2. The Argand plots for the S11 and P01 amplitudes from the final consistent resonances solutions for each channel showing the total partial wave amplitude from 1480 to 2170 MeV with ticks every integral multiple of 50 MeV (solid line) and the background term for each wave (dashed line) over the same energy range. The arrow indicates the direction of increasing energy.

most waves). Some exceptions are discussed in sect. 5 below, together with other results from these final solutions.

Throughout the fitting, the amplitude for each wave in each channel has been constrained to lie within the unitarity circle. For the final solutions we have checked *a posteriori* the combined channel unitarity condition

$$\text{Im } T_{\bar{K}N} \geqslant |T_{\bar{K}N}|^2 + |T_{\Sigma\pi}|^2 + |T_{\Lambda\pi}|^2$$

for each wave at 10 MeV c.m. energy intervals. With the exception of a few minor violations in the low partial waves below 1700 MeV, the condition is well satisfied by our solutions.

The amplitudes of these final solutions with the resonance parameters given in table 3, are presented every 10 MeV c.m. energy in table 4. The Argand diagrams are shown in fig. 1. To illustrate the simple background behaviour, fig. 2 shows the total amplitude and background component separately for two typical partial waves.

5. Discussion of the solutions

In this section the results obtained from the single channel fits and the final consistent resonance parameter fits are discussed for each wave. The resonance parameters are given in tables 2 and 3. Comparisons are also made with the results of previous analyses. In subsect. 5.3 the general form of our solutions is compared with the amplitudes obtained in other analyses.

5.1. The $I = 0$ waves

S01

The established S01(1670) with a large but simple background characterises this wave in both $\bar{K}N$ and $\Sigma\pi$ below ~1700 MeV. The mass of 1670 MeV and width of 45 MeV are determined from the $\Sigma\pi$ channel where pure I-spin data are available. The $\bar{K}N$ channel prefers a narrower width for this state (~25 MeV), but in the final stages of the fits the mass and width were fixed at the values from $\Sigma\pi$. Previous analyses report a wide range of values for the width and couplings of this state [26]. In the $\bar{K}N$ solution the S01 amplitude describes a broad anti-clockwise loop above 1700 MeV. This was parametrised as a resonance at 1825 MeV with a width of 250 MeV, resulting in improved fits to the total and channel cross sections and a very simple background. The effects of this broad resonance were seen only in the full range solutions.

In the $\Sigma\pi$ channel the background remains simple above 1700 MeV and no additional resonance is suggested. In particular a state at ~1825 MeV included in some of our preliminary solutions [12] does not satisfy the resonance criteria defined in sect. 4. However, a resonance amplitude in the $\Sigma\pi$ channel of 0.08 was obtained for the state found in the $\bar{K}N$ channel, but the background/resonance separation in the $\Sigma\pi$ channel is rather confused.

Several previous analyses have reported an S01 state between 1800 and 1900 MeV, as shown in fig. 4a, but there is no general agreement on the parameters of such a state.

P01

In both the $\bar{K}N$ and $\Sigma\pi$ channel two resonances are found in this wave, one at ~1570 MeV, the other at ~1850 MeV. These states were indicated in each channel independently, by the anti-clockwise movement of the amplitude when parametrised as pure background. Introducing the resonances resulted in a significant reduction in the χ^2 in the full range and the relevant short range solutions. In the final solutions with consistent resonances the mass and width values of 1573 MeV and 147 MeV for the lower state and 1853 MeV and 166 MeV for the upper state were acceptable in both channels, despite some differences between the best single channel values of these parameters (see table 2). As shown in fig. 4b some previous analyses have reported states ~1600 MeV and others claim states ~1750 MeV. We confirm the lower state but suggest that the higher state has a mass ~1850 MeV, this result being obtained when the lower state is also included.

P03

A resonance at 1900 MeV is required in the $\bar{K}N$ P03 amplitude to fit the RL-IC data [2] in this region. The χ^2 is reduced by about 120 when this state is introduced into the full range solution. Similarly structure in the $\Sigma^+\pi^-$ angular distributions at about 1900 MeV can only be explained by a resonance in P03. The $\Sigma\pi$ channel prefers a narrower width for this state, but the value was fixed to 70 MeV as determined from $\bar{K}N$.

The parameters obtained for P03(1900) are in good agreement with the results of

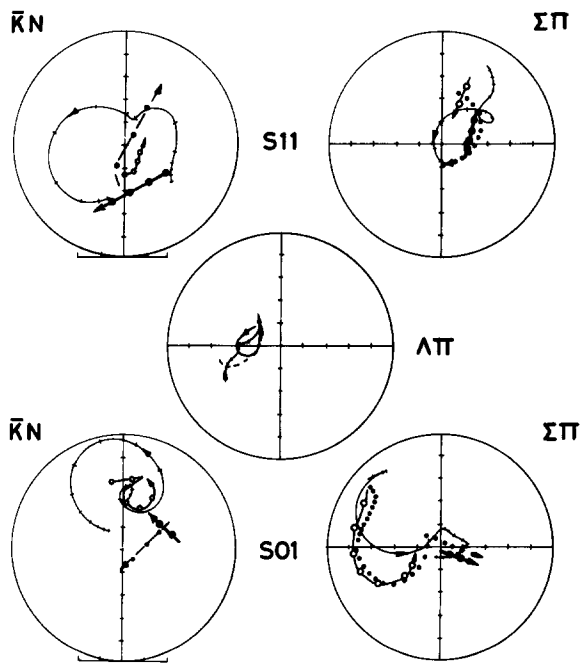

Fig. 3. (a) The Argand plots for the S01 and S11 partial wave amplitudes for the three channels from this analysis and from some previous analyses:

Analysis	Energy range	Channels shown	Ref.	Symbol
RLIC76	1480–2170	$\bar{K}N$, $\Sigma\pi$, $\Lambda\pi$	this paper	+++ *
Hemmingway et al.	1840–2220	$\bar{K}N$	[10]	-.-.-
CRS	1910–2170	$\bar{K}N$, $\Sigma\pi$	[11,5]	●—●—●
Kane	1540–2150	$\Sigma\pi$	[6]	.....
Baillon and Litchfield	1540–2150	$\Lambda\pi$	[18]	——— (soln. 1) – – – – (soln. 2)
CHS	1530–1700	$\bar{K}N$, $\Sigma\pi$	[21]	o—o—o

* Ticks every 50 MeV, first tick at 1500 MeV, last tick 2150 MeV.

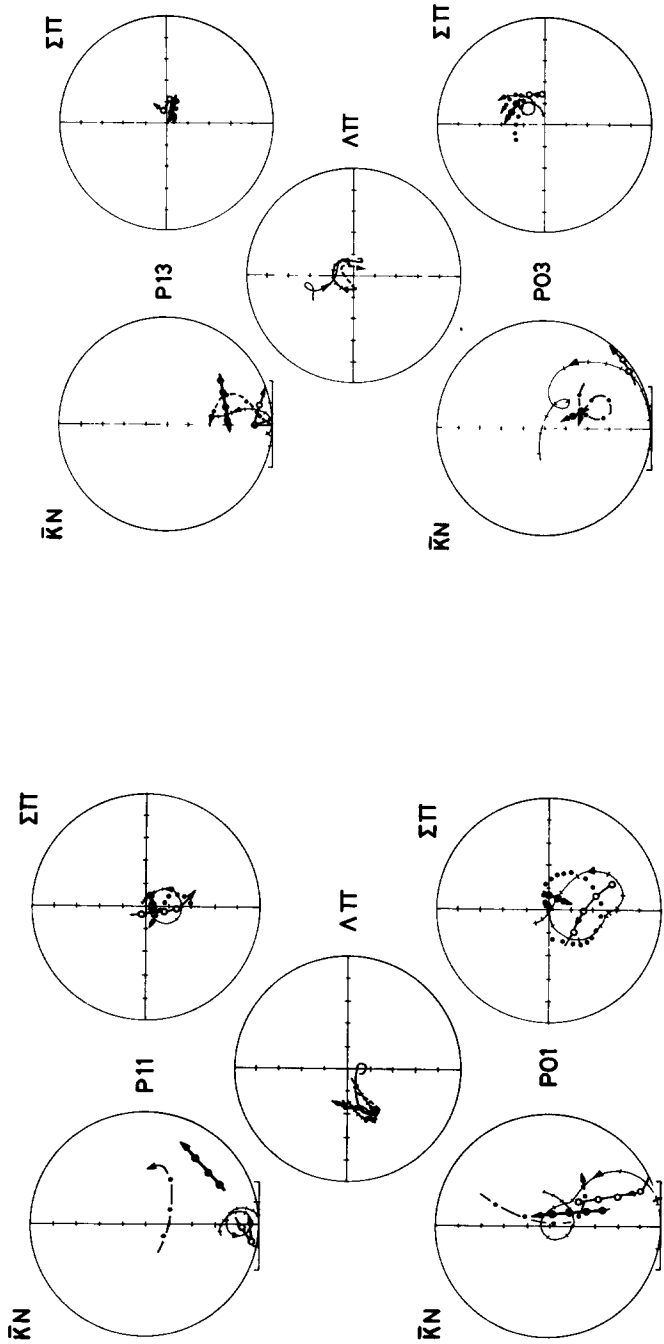

Fig. 3. (b) As fig. 3a for P01 and P11 amplitudes.

Fig. 3. (c) As fig. 3a for P03 and P13 amplitudes.

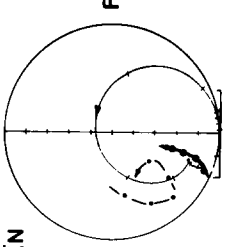

Fig. 3. (d) As fig. 3a for F05 and $\bar{K}N$ amplitudes.

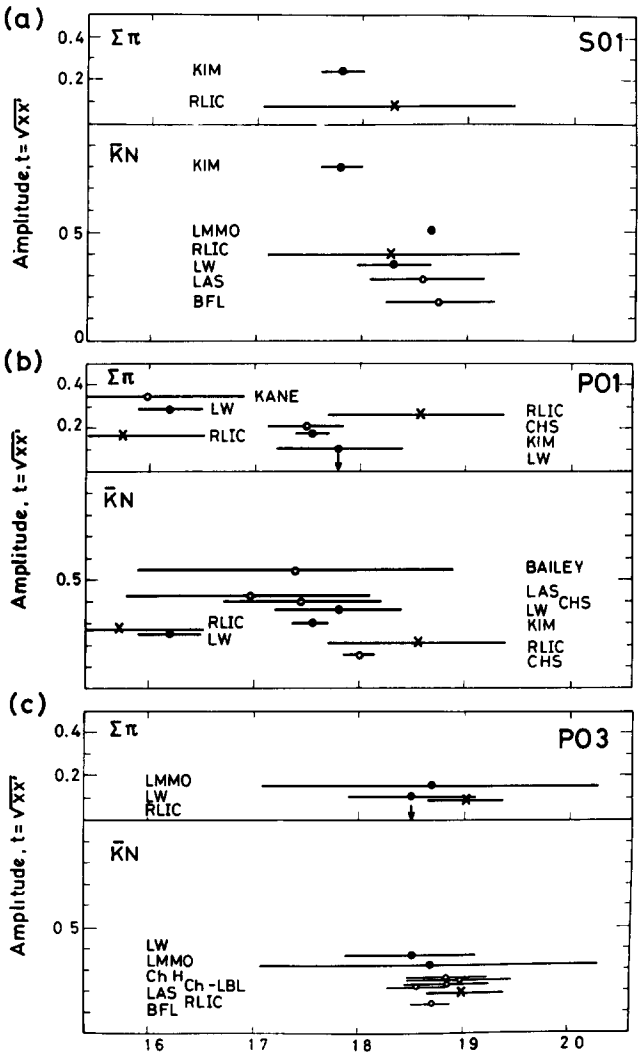
(a)
Σπ
S01
KIM
RLIC
K̄N
KIM
LMMO
RLIC
LW
LAS
BFL
Amplitude, t=√xx'
0.4
0.2
0.5
0
(b)
Σπ
P01
KANE
LW
RLIC
RLIC
CHS
KIM
LW
K̄N
BAILEY
LAS
CHS
LW
KIM
RLIC
CHS
RLIC
LW
(c)
Σπ
P03
LMMO
LW
RLIC
K̄N
LW
LMMO
Ch H
Ch-LBL
LAS
RLIC
BFL
16
17
18
19
20

Fig. 4 (a, b, c).

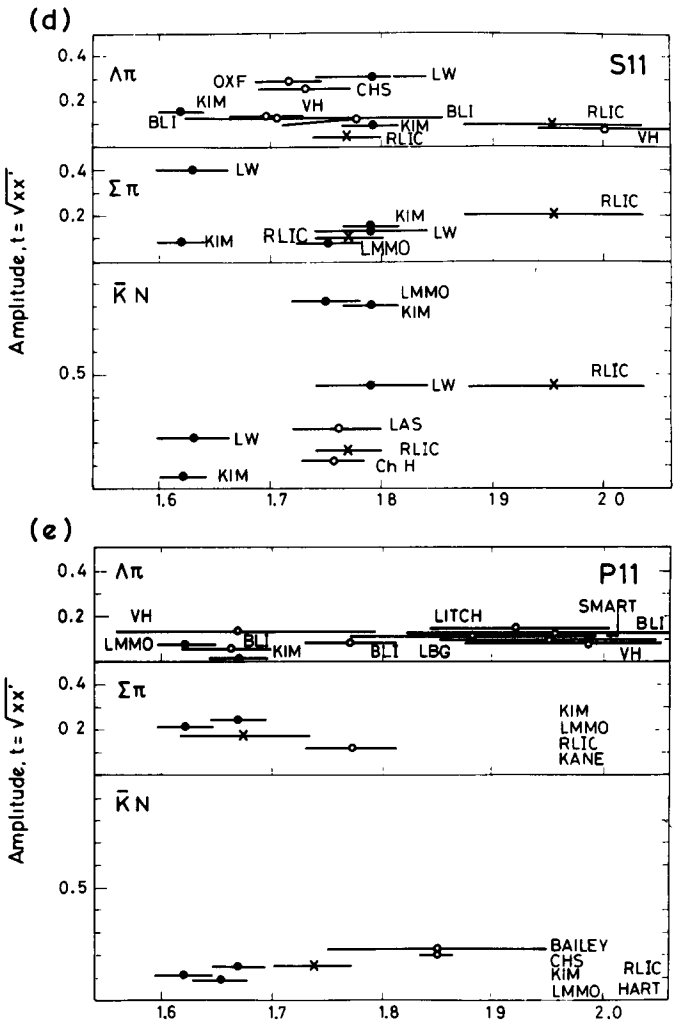

Fig. 4 (d,e).

Fig. 4. Resonant amplitude (ignoring sign) *versus* mass for the states claimed by previous analyses (indicated by an open circle for a single channel analysis and by a solid circle for a multichannel analysis), and found in this analysis (indicated by X). The horizontal bars represent the reported total widths. The comparisons are shown for the partial waves (a) S01, (b) P01, (c) P03, (d) S11, (e) P11. The entries are from the following references KIM [32], RLIC [this paper], LMMO [30], LW [33], LAS [34], BFL [35], KANE [6], CHS [13,19,21], Ch-H [10], OXF [36], VH [23], BL1 [18], BL2 [18], HART [37], BAILEY [38], LITCH [17], SMART [39]. (These figures are revised versions of those presented in a review by Plane [26].)

two previous analyses [10] as shown in fig. 4c. Since this state is now found independently in $\Sigma\pi$ it should be considered established.

D03

The established D03(1520) and D03(1690) dominate this wave below 1750 MeV in both $\bar{K}N$ and $\Sigma\pi$. The parameters of the D03(1520) are in excellent agreement with those obtained by Tripp [20]. As discussed in ref. [26] earlier results for D03(1690) have given width values between 25 and 77 MeV, elasticities between 0.14 and 0.28 and $\Sigma\pi$ amplitudes from -0.2 to -0.4. The width of 60 MeV obtained in our analysis has been stable throughout the solutions, constrained in $\Sigma\pi$ by new pure *I*-spin data in this region. The improved width determination led to a more reliable determination of the couplings.

Above 1750 MeV the D03 $\bar{K}N$ amplitude moves slowly with energy in an anti-clockwise direction and can be parametrised either as a background or as a broad resonance ($\Gamma \sim 350$ MeV) at the upper end of the energy range fitted. Since stable parameters were not obtained a resonance interpretation for this effect is dubious. In the $\Sigma\pi$ channel the D03 amplitude in this region is described by a simple background. The only previous claims for higher D03 states are one at 2010 MeV in [22] and a confused effect between 1935 and 2034 MeV in $\Lambda\omega$ [28].

D05

In the $\Sigma\pi$ channel the behaviour of this wave is described by the established D05(1825) with no background over the complete energy range fitted. The parameters of this resonance are now better determined with the new RL-IC [2] data in this region, the mass and width values obtained (1825 MeV and 94 MeV) being in the middle of the range of reported values [26].

In $\bar{K}N$ the D05 wave is parametrised as a simple, fairly large background. The D05(1825) was included in this wave with parameters fixed from $\Sigma\pi$, yielding a low elasticity of ~0.04.

F05

In both $\bar{K}N$ and $\Sigma\pi$ below ~1950 MeV this wave is dominated by the established F05(1822) resonance. The parameters of this state are very well determined from the $\bar{K}N$ channel, and were fixed at these values in the $\Sigma\pi$ channel. In the $\Sigma\pi$ solution this wave consistently described an anti-clockwise loop above 1950 MeV. This can be parametrised as a resonance at 2100 MeV with a width ~200 MeV, with no background. A similar but less obvious effect was observed in $\bar{K}N$. This could be parametrised as a resonance at ~2100 MeV as suggested from the $\Sigma\pi$ solution.

The F05(2100) state has been seen in two previous $\Sigma\pi$ analyses [5,6] using essentially the same data in this region and also confirmed by another recent analysis using new data above this energy range [29].

F07

In $\bar{K}N$ and $\Sigma\pi$ this wave is adequately described by a simple background. In $\bar{K}N$ a resonance with a mass ~2100 MeV and width ~100 MeV and coupling less than ~0.05 can be introduced in this wave, but this does not lead to an improved fit or simpler background. Similar observations follow from the $\Sigma\pi$ channel. We therefore

agree with the conclusion of ref. [10] that the data do not require this state, reported in two previous analyses [11,27].

G07

In the $\bar{K}N$ solution a small background is required under the established G07(2100), and as discussed in previous analyses [11] the width of this state is sensitive to the background assumed. Further the width is not well determined in this analysis since the state is close to the upper end of the energy range fitted. In $\Sigma\pi$ this wave requires a complicated background in addition to the G07(2100), but the background is simplified by introducing a non-zero resonance phase. The $\Sigma\pi$ data favour a narrower width for this state (~150 MeV) but this parameter is poorly determined and for the final fits was fixed to the value of 250 MeV obtained in the $\bar{K}N$ solution.

G09

In the final fits the high statistics K^-p elastic angular distributions from RL-IC collaboration [2] are poorly fitted in the region 1780 to 1835 MeV. The Legendre polynomial fits to these distributions indicate a significant A_7/A_0 coefficient peaking at about 1815 MeV, then becoming zero again at 1850 MeV then rising to a peak at about 2100 MeV. The upper peak is explained by the interference of the highly structured G07 and F17 amplitudes, but the peak at 1815 MeV is not predicted in any of our solutions. In particular interference of the dominant F05(1822) resonance with simple higher wave backgrounds were unable to explain this structure. Attempts were made to improve the fits to the angular distributions concerned by fitting the narrow energy region, 1780 to 1855 MeV, allowing only the background amplitude to vary for each wave in turn up to H19. Only the G09 and G19 waves improved the fits to these distributions, but the amplitudes had changed drastically from the long range solution values. It was impossible to extend these solutions to a longer energy range with a simple continuous G09 or G19 background. For this reason the fits were repeated over the angular distributions concerned trying a narrow resonance at ~1810 MeV in each wave. Such a resonance in either of the G9 waves significantly improves the fits to the K^-p elastic angular distributions, but a G19 resonance worsens the fits to the $K^-p \to \bar{K}^0n$ distributions. When a G09 resonance at 1808 MeV with a width of 27 MeV and an elasticity of 4% is included in the long range solution the χ^2 to the distributions concerned improves from 151 to 119 for 120 data points. Thus this state is probable by the criteria in sect. 4. However we are aware that a $\frac{9}{2}$ state at this mass is unexpected and therefore, subsequent to the partial wave analyses a further independent investigation of possible data biases was made but no spurious source of the effect has been found. It is stressed that the inclusion of the G09 state does not affect the other partial waves.

There is no evidence for a G09(1808) in the $\Sigma\pi$ channel; all waves with $J \geqslant \frac{9}{2}$ were consistent with zero.

H09

In $\bar{K}N$ this wave is described by a small simple background.

5.2. The I = 1 waves

S11

In $\bar{K}N$ two S11 resonances are found one at 1770 MeV and the other at 1955 MeV. Both these were indicated by the anti-clockwise movement of this wave when parametrised as pure background. The quality of the fit was improved when each of the resonances was introduced, and with both resonances in this wave the background was reduced to a very simple form, shown in fig. 2.

In $\Sigma\pi$ a resonance was required at about 1900 MeV, with width ~100 MeV to fit the $\Sigma^+\pi^-$ cross section but no other S11 resonances are indicated. At least two resonances are indicated in this wave in $\Lambda\pi$, although the structure in this wave is confused. A lower state is suggested at ~1720 MeV with a width of ~70 MeV. The mass of the higher state is unstable varying between 1815 and 1960 MeV in different fits. In later stages of the fitting the mass was fixed at the value obtained from the corresponding state in $\bar{K}N$.

In the final solutions with consistent resonances, parameters were obtained in the three channels for the two S11 states without causing a significant increase in χ^2 despite the considerable difference for example for the S11(1955) width obtained from the best single channel fits. The S11(1770) was accepted in the $\Sigma\pi$ solution with an amplitude at resonance of 0.09, but with considerable background. In the final $\Lambda\pi$ solution it is not clear that the S11(1770) represents the same effect as that at 1720 MeV found in the single channel solution. Better data are required in this region to really sort out the structure.

Fig. 4d shows the previous results for S11 resonances. A state in the region of 1770 MeV is found in many analyses, but there is no agreement concerning the elasticity and $\Lambda\pi$ couplings of this state, reflecting the confusion mentioned above. Ref. [18] reports two possible S11 states in this region, one at 1700 MeV, the other at 1780 MeV in different ambiguous $\Lambda\pi$ solutions.

The higher state at 1955 MeV required by our solution has not been seen in previous analyses, but may correspond to the state at 2004 MeV reported by Van Horn [23] in $\Lambda\pi$.

P11

In the $\Sigma\pi$ solutions this wave showed resonance like behaviour and was parametrised as a resonance at 1680 MeV with a width of 120 MeV with a very small background. The evidence for this state comes mainly from the $K^0_L p \to \Sigma^0\pi^+$ data. This state was searched for in the $\bar{K}N$ channel but the high precision total cross section data required a P11 state at 1740 MeV. In the final solutions we were unable to find common parameters for a P11 in $\bar{K}N$ and $\Sigma\pi$ without producing a large increase in χ^2, suggesting that these effects may indicate the existence of two P11 states in this region, although the $\bar{K}N$ result relies mainly on preliminary cross section data [3a]. Attempts to include both P11 states in either channel were unsuccessful.

In $\Lambda\pi$ the P11 wave is parametrised as a complicated background that shows a

sharp reversal at about 1900 MeV. No P11 states in the region of 1700 MeV were required or accepted in the $\Lambda\pi$ solution. Previous $\Lambda\pi$ solutions have claimed various P11 states, as shown in fig. 4e, but with no general agreement although Baillon and Litchfield [18] and Van Horn [23] claim P11 states ~1700 MeV that may correspond to our $\bar{K}N$ or $\Sigma\pi$ results. Claims for P11 states in previous $\bar{K}N$ and $\Sigma\pi$ analyses are similarly diverse. We find no evidence for a higher P11 ~1900 MeV claimed by several previous analyses (see fig. 4e).

P13

The P13 wave is notable for its simplicity and lack of any resonance behaviour in all three channels. In $\bar{K}N$ the P13 amplitude describes a slow anti-clockwise movement below 1750 MeV then continues approximately linearly. Attempts to replace the structure with a broad resonance were unsuccessful. In $\Sigma\pi$ the wave shows very little energy variation over the complete energy range and in $\Lambda\pi$ the amplitude describes a slow clockwise loop in the Argand diagram. This complete lack of P13 states below ~2100 MeV is a feature consistent with almost all previous analyses.

D13

The established D13(1670) is clear in all three channels and the parameters are well determined in the $\Sigma\pi$ and $\Lambda\pi$ solutions, yielding consistent values of mass of 1670 ± 5 MeV and width of 50 ± 5 MeV. The major constraint in $\Sigma\pi$ comes from the pure $I = 1$, $\Sigma^0\pi^+$ data. Above about 1750 MeV in $\Sigma\pi$ and $\Lambda\pi$ the D13 amplitude describes an anti-clockwise loop. In the $\Sigma\pi$ solutions this can be parametrised as a broad resonance at ~1900 MeV and in $\Lambda\pi$ by a resonance at 1986 MeV, leading to a simpler background in both channels. In the final fits the effects in both channels were attributed to a resonance at 1920 MeV with a width of 300 MeV. In the $\bar{K}N$ a background is required in this wave but no resonance is indicated and when a D13(1920) was introduced into the final solutions an elasticity of <0.03 was obtained. Several previous analyses of $\Lambda\pi$ [17,23,18,27] have reported a D13 state ~1950 MeV with resonant amplitudes between 0.04 and 0.14 and two earlier $\Sigma\pi$ [6,27] analyses have reported this state. The only claim for such a state in $\bar{K}N$ comes from the multichannel analysis of ref. [30].

Due to the energy spacing of the fitted data, our analyses are not sensitive to states with $\Gamma \lesssim 20$ MeV and hence would not see the $\Sigma(1580)$ reported from total cross section measurements [3a] and identified as D13(1580) by a re-examination of the CHS $\Lambda\pi$ data in smaller energy bins by Litchfield [31]. Further, the D13(1580) is accomodated only in solution I of ref. [18], whereas our $\Lambda\pi$ solution corresponds to their solution II as discussed in subsect. 5.3.

D15

In all three channels this wave is dominated by the established D15(1774), but a simple background is required above ~1800 MeV in each case. The parameters of this state are well determined in our solutions, favouring a rather higher mass and width than some previous analyses (1774 MeV and 130 MeV compared with averages from ref. [26] of 1765 MeV and 110 MeV, respectively). No other resonances are indicated in this wave.

F15

The established F15(1920) is found in all three channels, but this state has a low elasticity (0.05 ± 0.03) and the parameters were taken from the $\Sigma\pi$ solution.

In $\Lambda\pi$ the parameters of this state are not well determined due to the correlation between this wave and the S11, P11 and D13 waves which are all active in this region. However when the mass was fixed at the $\Sigma\pi$ value a width of 121 MeV was obtained for this state, consistent with the $\Sigma\pi$ results. Previous $\Lambda\pi$ analyses have reported narrower widths for this state, between 50 and 102 MeV, inconsistent with the higher values reported from $\Sigma\pi$ analyses.

In all three channels there is a simple background in this wave. In $\Sigma\pi$ this describes a broad anti-clockwise loop similar to the behaviour of the F05 $\Sigma\pi$ amplitude. The behaviour of F15 and F05 above 1950 MeV in $\Sigma\pi$ was carefully investigated in both long and short range solutions. Stable resonance parameters for the F15 effect could not be obtained, suggesting that a resonance interpretation as claimed in ref. [5] is unjustified with the present data.

F17

The established F17(2040) is seen clearly in all three channels. The parameters of this state are well determined in the $\bar{K}N$ and $\Lambda\pi$ channels and are in fair agreement with previous results. A simple background is required in each channel.

G17

In $\bar{K}N$ and $\Lambda\pi$ this wave is described by a small and simple background. In $\Sigma\pi$ the G17 amplitude exhibits a slow anti-clockwise movement on the Argand diagram at the upper end of the energy range fitted, but a resonance interpretation cannot be claimed.

G19, H19

These waves are very small throughout the energy region of these analyses. Neither was required in the $\Sigma\pi$ analyses and H19 was set to zero in the $\Lambda\pi$ analysis.

5.3. Comparisons with previous solutions

Comparing our solutions with those of previous analyses, two classes of discrepancies are observed. In some cases different analyses agree on the general form of a partial wave but can obtain different resonance results due to the form of parametrisation, resonance criteria and the data fitted. In other cases completely different forms of amplitudes are obtained for certain partial waves, indicating the existence of ambiguous solutions. The comparisons with the analyses of Hemmingway et al. [10] ($\bar{K}N$), Kane [6] ($\Sigma\pi$), CRS [5,11] ($\bar{K}N$, $\Sigma\pi$), Baillon and Litchfield [18] ($\Lambda\pi$), CHS [19,21] ($\bar{K}N$, $\Sigma\pi$) and Tripp [20] ($\bar{K}N$, $\Sigma\pi$) can be summarised as follows:

(a) There is general agreement concerning the form of the amplitudes of the higher partial waves ($J \geqslant \frac{5}{2}$) in all three channels, although as shown in fig. 3 there is some disagreement in the behaviour of the $\bar{K}N$ F05 amplitude above 1900 MeV.

(b) In the region of 1520 MeV, where $\bar{K}N$ and $\Sigma\pi$ solutions are dominated by D03(1520), the low waves of our $\bar{K}N$ and $\Sigma\pi$ solutions are in good agreement with those of Tripp [20].

(c) The $\Lambda\pi$ solution is similar in all waves to the simpler of the two ambiguous solutions (solution II) of Baillon and Litchfield [18] and the energy dependent solutions of Van Horn [23].

(d) In $\Sigma\pi$ there is a fair agreement in all waves with the solutions referenced above although new $I = 1$ data [7] and the use of a non-zero phase parameter for the S01(1670) leads to some differences in the $J = \frac{1}{2}$ waves, as illustrated in fig. 3.

(e) In the $\bar{K}N$ channel, inspection of the low wave Argand diagrams shows that several different solutions have been found by previous analyses and continuity between the lower energy and higher energy solutions is poor, particularly in the $J = \frac{1}{2}$ waves, (as shown in fig. 3). Our amplitudes are in fair agreement with the low energy solutions of CHS [21]. At the higher energies however the amplitudes for the $J = \frac{1}{2}$ waves are completely different from those of Hemmingway et al. [10] or of CRS [11]. Minor discrepancies are also observed in the $J = \frac{3}{2}$ amplitudes.

The discrepancy in $\bar{K}N$ noted in (e) above illustrates that with similar assumptions different solutions can be obtained over shorter energy ranges. Using an energy semi-independent approach Baillon and Litchfield [18] obtained two solutions for the $\Lambda\pi$ channel between 1540 and 1750 MeV and essentially a unique solution from 1750 to 2150 MeV, by applying the conditions of minimum structure and fixed resonant amplitudes for the D15 and F17 waves. If such conditions are relaxed, many ambiguous solutions are possible as was demonstrated for the same channel by Van Horn [31] using the formalism of Barrellet zeros. Similar investigations of the possible ambiguities of the more complicated $\bar{K}N$ and $\Sigma\pi$ solutions should be performed. However it is clear that by imposing reasonable physical assumptions the large number of possible ambiguous solutions is then reduced to a few acceptable solutions. The number obtained depends critically on the assumptions made, such as the simplicity of the behaviour of the partial wave amplitudes, the resonance assumptions and the order at which the partial wave expansion is truncated.

With the conditions that the solutions (a) exhibit simple continuity as imposed by our partial wave parametrisation over the wide energy range 1480 to 2170 MeV, which includes the region of ~1520 MeV where the solutions are particularly simple, (b) show consistent resonance structure in the three channels, and (c) include the established resonances, we have found only one solution for each channel.

5.4. Classification of Y's*

The classification of baryon resonances in terms of levels in an harmonic oscillator quark model and analyses of decay rates in terms of $SU(6)_W$ schemes have been discussed in detail in previous publications (e.g. refs. [24,25]). By checking decay amplitude signs for the Y^* states from our analyses the following observations can be made.

(a) The $\frac{1}{2}^-$ states $\Lambda(1825)$, $\Sigma(1955)$ and $\Sigma(1770)$ and the $\frac{3}{2}^-$ $\Sigma(1920)$ fit into the $N = 1$, $(70, 1^-)$ SU(6) multiplet, leaving only two Y^* states in this multiplet for which there are no candidates. (In this notation (M, LP), M is the SU6 multiplicity,

L the orbital angular momentum of the three quark system which couples with total quark spin $\frac{1}{2}$ or $\frac{3}{2}$ to give the spin J of the state, and P is the intrinsic parity. The principle quantum number of the harmonic oscillator level is N.)

(b) The P03 $\Lambda(1900)$ fits well in the $N = 2$, $(56, 2^+)$ multiplet, the sign of the $\Sigma\pi$ being as predicted. There are however several Y^* states required to complete this multiplet.

(c) In the $N = 2$ $(56, 0^+)$ levels the $\frac{1}{2}^+$ $\Lambda(1573)$ and $\Sigma(1676)$ found in our analyses are partners for the N(1470). The Σ member of the $\frac{3}{2}^+$ decuplet in this multiplet is still missing.

(d) Evidence for the existence of the $N = 2$, $(70, 2^+)$ and $(70, 0^+)$ multiplets is weak as discussed in ref. [25]. However the existence of a F05 $\Lambda(2100)$ state with positive $\Sigma\pi$ coupling can only be accomodated in a $(70, 2^+)$. The confirmation of this state is thus a crucial test for the existence of the $(70, 2^+)$ $N = 2$ levels. There is no evidence from the Y^*'s for the $(70, 0^+)$ $N = 2$ multiplet.

(e) The lowest multiplet that could accomodate the $\frac{9}{2}^-$ $\Lambda(1808)$ state found in our $\bar{K}N$ analysis is the $(70, 3^-)$ $N = 3$ system. However the mass of this state is much lower than would be expected for this multiplet, of which $\frac{7}{2}^-$ $\Lambda(2100)$ is a singlet member.

(f) Apart from the G09 $\Lambda(1808)$ state all the Y^* states found in our analyses are easily accomodated in the quark model SU6 multiplets. In particular no $\frac{5}{2}^-$ Y^* states apart from the established $\Lambda(1825)$ and $\Sigma(1774)$ are found below 2170 MeV.

6. Summary

Using a carefully selected set of the most recent $\bar{K}N$ data, energy dependent partial wave solutions to the reactions $\bar{K}N \to \bar{K}N$, $\bar{K}N \to \Sigma\pi$ and $\bar{K}N \to \Lambda\pi$ have been found. These partial waves parametrised as a sum of resonances and simple backgrounds fit the data well over the wide energy range 1480 to 2170 MeV. Consistent resonance structure has been obtained in the three channels, giving a better determination of the parameters of the established states, confirming several other states and providing evidence for two new states. With the condition of simple energy continuity and consistent resonance structure only one solution was found for each channel.

The conventional high statistics bubble chamber data in the region between 1480 and 1530 MeV and above 1730 MeV have led to a better determination of the partial waves. New data with equivalent statistics in the region 1530 to 1730 MeV could solve some of the uncertainties in the partial wave amplitudes in this region. Data from the pure isospin-1 channel, $K^0_L p \to \Sigma^0\pi^+$ [7] have helped to separate the $I = 0$ and $I = 1$ effects in the region 1530 to 1700 MeV. More data from this channel or other pure isospin channels (e.g. $K^-n \to \Sigma\pi$) would remove some uncertainties in the solutions, particularly at the higher energies. Polarisation measurements are required for K^-p elastic scattering below 1720 MeV where no data are available. Fi-

nally, as stated by many previous authors, measurements of R and A parameters and better polarisation measurements in various channels are required.

We wish to thank W. Cameron for performing the additional data checks mentioned in subsect. 5.1, R. Kelly for preparing the Argand diagrams of fig. 1 and G.E. Kalmus for many helpful discussions throughout the work of these analyses.

References

[1] R.D. Tripp, private communication;
T.S. Mast, M. Alston-Garnjost, R O. Bangerter, A.S. Barbaro-Galtieri, F.T. Solmitz and R.D. Tripp, Phys. Rev. D11 (1975) 3078.
[2] RL-IC Collaboration, B. Conforto, G.P. Gopal, G.E. Kalmus, P.J. Litchfield, R.T. Ross, A.J. Van Horn, T.C. Bacon, I. Butterworth, E.F. Clayton and R.M. Waters, Nucl. Phys. B105 (1976) 189.
[3] K.K. Li, Baryon resonances 1973 (Purdue University) p. 283;
D. Michael and T. Kycia, private communications,
D.V. Bugg, R.S. Gilmore, K.M. Knight, D.C. Salter, G.H. Stafford, E.J.N. Wilson, J.D. Davies, J.D. Powell, P.M. Hattersley, R.J. Homer, A.W. O'Dell, A.A. Carter, R.J. Tapper and K.F. Riley, Phys. Rev. 168 (1968) 1466.
[4] P. Baillon, C. Bricman, M. Ferro-Luzzi, J.M. Perreau, R.D. Tripp, T. Ypsilantis, Y. Declais and J. Seguinot, Phys. Letters 50B (1974) 377, 383; CERN 75-10, unpublished.
[5] A. Berthon, J. Vrana, I. Butterworth, P.J. Litchfield, J.R. Smith, J. Meyer, E. Pauli and B. Tallini, Nucl. Phys. B24 (1970) 417.
[6] D.F. Kane, Phys. Rev. D5 (1972) 1583; LBL-2452 (1974), unpublished.
[7] BEGPR Collaboration, L. Bertanza, W. Cameron, P. Capiluppi, P. Croft, E. Flaminio, R. Jennings, G. Kalmus, P. Lugaresi-Serra, G. Mandrioli, A. Minguzzi-Ranzi, W. Morton, A. Nappi, R. Pazzi, K.J. Peach, A.M. Rossi, B. Saitta and W. Venus, RL-76-016.
[8] J.M. Blatt and V.F. Weisskopf, Theoretical nuclear physics (Wiley, New York, 1952) p. 361.
[9] A.J. Van Horn, Apple program users' guide (R.L. Bubble Chamber Group Physics Note no. 83 – 1974) unpublished.
[10] B. Conforto, D.M. Harmsen, T. Lasinski, R. Levi-Setti, M Raymund, E. Burkhardt, H. Filthuth, S. Klein, H. Oberlack and H. Schleich, Nucl. Phys. B34 (1971) 41;
R.J. Hemmingway, J. Eades, D.M. Harmsen, J.O. Petersen, A. Putzer, C. Kiesling, D.E. Plane and W. Wittek, Nucl. Phys. B91 (1975) 12.
[11] P.J. Litchfield, T.C. Bacon, I. Butterworth, J.R. Smith, E. Lesquoy, R. Strub, A. Berthon, J. Vrana, J. Meyer, E. Pauli, B. Tallini and J. Zatz, Nucl. Phys. B30 (1971) 125.
[12] Rutherford Laboratory - Imperial College Collaboration, Palermo Conf. 1975;
R.T. Ross, New results on $S = \pm 1$ baryons, RL-75-115 and Proc. Palermo Conf., 1975.
[13] R. Armenteros, P. Baillon, C. Bricman, M. Ferro-Luzzi, E. Pagiola, J.O. Petersen, D.E. Plane, N. Schmitz, E. Burkhardt, H. Filthuth, E. Kluge, H. Oberlack, R.R. Ross, R. Barloutaud, P. Granet, J. Meyer, J.P. Porte and J. Prevost, Nucl. Phys. B21 (1970) 15;
R. Armenteros, M. Ferro-Luzzi, D.W G.S. Leith, R. Levi-Setti, A. Minten, R.D. Tripp, H. Filthuth, V. Hepp, E. Kluge, H. Schneider, R. Barloutaud, P. Granet, J. Meyer and J.P. Porte, Nucl. Phys. B8 (1968) 233.
[14] M. Jones, R. Levi-Setti, D. Merrill and R.D. Tripp, Nucl. Phys. B90 (1975) 349.
[15] CERN-Heidelberg Collaboration, paper presented by P. Baillon at 2nd Aix-en-Provence Conf., 1973.

[16] C. Daum, F.C. Erné, J.P. Lagnaux, J.C. Sens, M. Steuer and F. Udo, Nucl. Phys. B6 (1968) 273;
S. Andersson-Almehed, C. Daum, F.C. Erné, J.P. Lagnaux, J.C. Sens and F. Udo, Nucl. Phys. B21 (1970) 515,
M.G. Albrow, S. Andersson-Almehed, B. Bosnjakovic, F.C. Erné, Y. Kimura, J.P. Lagnaux, J.C. Sens and F. Udo, Nucl. Phys. B29 (1971) 413;
C.R. Cox, P.J. Duke, K.S. Heard, R.E. Hill, W.R. Holley, D.P. Jones, F.C. Shoemaker, J.J. Thresher, J.B. Warren and J.C. Sleeman, Phys. Rev. 184 (1969) 1443.
[17] P.J. Litchfield, Nucl. Phys. B22 (1970) 269.
[18] P. Baillon and P.J. Litchfield, Nucl. Phys. B94 (1975) 39.
[19] R. Armenteros, P. Baillon, C. Bricman, M. Ferro-Luzzi, D.E. Plane, N. Schmitz, E. Burkhardt, H. Filthuth, E. Kluge, H. Oberlack, R.R. Ross, R. Barloutaud, P. Granet, J. Meyer, J.P. Porte and J. Prevost, Nucl. Phys. B8 (1968) 223.
[20] R.D. Tripp, UCRL 19765 (1970), unpublished.
[21] R. Armenteros, P. Baillon, C. Bricman, M. Ferro-Luzzi, D.E. Plane, N. Schmitz, E. Burkhardt, H. Filthuth, E. Kluge, H. Oberlack, R.R. Ross, R. Barloutaud, P. Granet, J. Meyer, J.P. Porte and J. Prevost, Nucl. Phys. B14 (1969) 91.
[22] Particle Data Group, Review of particle properties, Phys. Letters 50B (1974) 1.
[23] A.J. Van Horn, Nucl. Phys. B87 (1975) 145.
[24] R. Horgan and R.H. Dalitz, Nucl. Phys. B66 (1973) 135.
[25] A.J. Hey, P.J. Litchfield and R.J. Cashmore, Nucl. Phys. B95 (1975) 516.
[26] D.E. Plane, Baryon resonances 1973 (Purdue University, 1973) p. 253.
[27] A. Barbaro-Galtieri, Hyperon resonances 1970 (Duke University, 1970) p. 173.
[28] A. Brandstetter, I. Butterworth, S.M. Deen, P.J. Litchfield, A. Berthon, J. Vrana, J. Zatz, W. Wojcik, J. Meyer and B. Tallini, Nucl. Phys. B39 (1972) 13.
[29] A. de Bellefon, P. Billoir, A. Berthon, J.M. Brunet, S. Tristram, J. Vrana, B. Buccari, G. Poulard and B. Tallini, Saclay preprint D. Ph. PE-76-03 (1976).
[30] A. Lea, B. Martin, R. Moorhouse and G. Oades, Nucl. Phys. B56 (1973) 77.
[31] A.J. Van Horn, Nucl. Phys. B87 (1975) 157.
[32] J.K. Kim, Phys. Rev. Letters 27 (1971) 356.
[33] W. Langbein and F. Wagner, Nucl. Phys. B47 (1972) 477.
[34] T.A. Lasinski, Nucl. Phys. B29 (1971) 125.
[35] C. Bricman, M. Ferro-Luzzi and J.P. Lagnaux, Phys. Letters 33B (1970) 511.
[36] D. Baxter, I. Buckingham, I. Corbett, P. Dunn, J. Emmerson, A. Engler, J. Garvey, F. Hart, G. Hughes, C. Jones, R. Maybury, N. Middlemass, P. Norton, J. Scheid, A. Segar and T. Quirk, Baryon resonances 1973 (Purdue University, 1973) p. 315.
[37] E.L. Hart, R.M. Rice, R.B. Bacastow, S.Y. Fung, S.S. Hertzbach, R. Ponte, J. Button-Shafer, S.S. Yamamoto and D.A. Evans, Baryon resonances 1973 (Purdue University, 1973) p. 311.
[38] D.S. Bailey, UCRL-50617 (1969).
[39] W.M. Smart, Phys. Rev. 169 (1968) 1330.